

RESEARCH ARTICLE

10.1029/2018JB015805

Key Points:

- The Myanmar jadeitites have $\delta^{26}\text{Mg}$ values lower than normal mantle
- Jadeite-forming fluids have high contents of Na-Al-Si and low Mg contents and $\delta^{26}\text{Mg}$ values
- Subduction zone fluids at forearc depths may have low $\delta^{26}\text{Mg}$ values due to carbonate dissolution

Supporting Information:

- Supporting Information S1

Correspondence to:

Y. Chen and F. Huang,
chenyi@mail.iggcas.ac.cn;
fhuang@ustc.edu.cn

Citation:





Chen, Y., Huang, F., Shi, G.-H., Wu, F.-Y., Chen, X., Jin, Q.-Z., et al. (2018). Magnesium isotope composition of subduction zone fluids as constrained by jadeitites from Myanmar. *Journal of Geophysical Research: Solid Earth*, 123. <https://doi.org/10.1029/2018JB015805>

Received 21 MAR 2018

Accepted 2 SEP 2018

Accepted article online 5 SEP 2018

Magnesium Isotope Composition of Subduction Zone Fluids as Constrained by Jadeitites From Myanmar

Yi Chen^{1,2,3} , Fang Huang⁴ , Guang-Hai Shi⁵ , Fu-Yuan Wu^{1,2}, Xi Chen⁴, Qi-Zhen Jin⁴, Bin Su¹, Shun Guo^{1,2}, Kyaing Sein⁶, and Thet Tin Nyunt⁷ 

¹State Key Laboratory of Lithospheric Evolution, Institute of Geology and Geophysics, Chinese Academy of Sciences, Beijing, China, ²CAS Center for Excellence in Tibetan Plateau Earth Sciences, Beijing, China, ³College of Earth and Planetary Sciences, University of Chinese Academy of Sciences, Beijing, China, ⁴Geochemistry Department of Human Resources, University of Science and Technology of China, Hefei, Anhui, China, ⁵State Key Laboratory of Geological Processes and Mineral Resources, China University of Geosciences, Beijing, China, ⁶Myanmar Geosciences Society, Hlaing University Campus, Yangon, Myanmar, ⁷Department of Geology, University of Yangon, Yangon, Myanmar

Abstract Subduction zone fluids are critical for transporting materials from subducted slabs to the mantle wedge. Jadeitites from Myanmar record fluid compositions and reactions in the forearc subduction channel. Here we present high-precision Mg isotope data of the Myanmar jadeitites and associated rocks to understand the Mg isotope composition of subduction zone fluids at forearc depths. Two types of jadeitites (white and green) exhibit distinct Mg isotope compositions. The white jadeitites precipitated from Na-Al-Si-rich fluids and have low $\delta^{26}\text{Mg}$ values, varying from -1.55‰ to -0.92‰ , whereas the green jadeitites have higher $\delta^{26}\text{Mg}$ values (-0.91‰ to -0.74‰) due to metasomatic reactions between fluids and Cr spinel. The amphibole-rich blackwall in the contact boundaries between jadeitites and serpentinites also exhibits low $\delta^{26}\text{Mg}$ values (-1.17‰ to -0.72‰). Therefore, the jadeite-forming fluids have not only high concentrations of Na-Al-Si but also low $\delta^{26}\text{Mg}$ values. The low $\delta^{26}\text{Mg}$ signature of the fluids is explained by the dissolution of Ca-rich carbonate in subducted sediments or altered oceanic crust, which is supported by the negative correlation of $\delta^{26}\text{Mg}$ with CaO/TiO₂, CaO/Al₂O₃, and Sr in the white jadeitites. Given the common occurrence of Ca-rich carbonates in the subduction channel, the Mg isotope composition of low-Mg aqueous fluids would be significantly modified by dissolved carbonates. Metasomatism by such fluids along conduits has the potential to generate centimeter-scale Mg isotope heterogeneity in the forearc mantle wedge. Therefore, Mg isotopes could be a powerful tracer for recycled carbonates not only in the deep mantle but also in the shallow regions of subduction zones.

1. Introduction

The subduction of oceanic lithosphere has long been recognized as a key process in recycling large amounts of fluids into the mantle (e.g., Bebout, 2013; Hermann et al., 2006; Manning, 2004; Schmidt & Poli, 1998). The fluids derived from the dehydration of subducted slabs can change the mantle chemical-physical properties including volatile contents, trace element abundances, radiogenic isotope systematics, seismic velocities, and electrical conductivities (Hyndman & Peacock, 2003; Morris & Ryan, 2003). Arc volcanism in convergent plate margins is commonly linked to the fluids released into the mantle wedge (e.g., Elliott et al., 1997; Plank & Langmuir, 1993; Tatsumi, 1989). Furthermore, the residual descending slab could also reserve some fluids in hydrous or nominally anhydrous minerals and influence the chemical composition of the deep mantle, which may subsequently contribute to the source material of intraplate basalts (Hofmann, 1997).

Sediments and oceanic crust in subducted slabs have been identified as the major reservoirs delivering fluid-mobile elements to the overlying mantle wedge (e.g., Elliott, 2003; Spandler & Pirard, 2013). Serpentinites are also an important reservoir for volatiles and fluid-mobile elements (Scambelluri et al., 2004, 2015; Spandler et al., 2014). The contributions of slab fluid sources (such as metamorphosed basalt, sediment, and serpentine) can be identified based on the trace element and isotope compositions of subduction-related magmas (e.g., King et al., 2006; Marschall & Schumacher, 2012; Spandler & Pirard, 2013).

Unlike many incompatible trace elements and radiogenic isotopes, the Mg isotope composition of mantle wedge peridotites are insensitive to metasomatism and partial melting processes because the Mg

concentrations of slab-derived fluids are significantly lower than those of mantle peridotites. However, recent studies have revealed that some arc lavas have slightly higher $\delta^{26}\text{Mg}$ values relative to the normal mantle (Li et al., 2017; Teng et al., 2016), whereas some cratonic eclogites and subduction-related basalts have lower $\delta^{26}\text{Mg}$ values (Huang, Li et al., 2015; Li et al., 2017; Wang et al., 2012, 2015; Yang et al., 2012). These observations raise an important question on the mechanisms for transferring the heterogeneous Mg isotope signatures of the recycled slabs to the mantle. Determining the Mg isotope composition of subduction zone fluids can place critical constraints on this recycling process (Chen et al., 2016; Wang et al., 2017). However, there are no experimental calibrations or direct measurements of Mg isotope data from subduction zone fluids, which hampers our understanding of the above question.

Jadeitite is a rare high-pressure/low-temperature metamorphic rock composed almost entirely of jadeite ($\text{NaAlSi}_2\text{O}_6$), which is commonly associated with oceanic blueschists and eclogites in serpentinite mélanges (Harlow et al., 2015; Schertl et al., 2012; Tsujimori & Harlow, 2012). Jadeitite samples directly record fluid activities in the subduction channel (Harlow et al., 2015; Shi et al., 2012; Tsujimori & Harlow, 2012) and thus offer a window into the geochemical processes of fluid-related mass transfer within oceanic subduction zones (Harlow et al., 2016). The Jade Mine Tract from Kachin State in northwestern Myanmar is the largest jadeitite (jade) deposit in the world. Intensive studies have demonstrated that the Myanmar jadeitites represent either the direct aqueous fluid precipitate (P-type) from slab dehydration into the mantle wedge (Shi et al., 2009, 2012; Sorensen et al., 2006) or the metasomatic replacement (R-type) of crustal protoliths by fluid-rock interaction (Lei et al., 2016; Yui et al., 2013). Therefore, the Myanmar jadeitites provide an excellent opportunity to study the Mg isotope composition of subduction zone fluids.

In this study, we provide precise Mg isotope data for jadeitites and associated rocks, including amphibole-rich blackwalls and serpentinites collected from the serpentinite mélange at the Myanmar Jade Mine Tract. The purpose of this study is to constrain the Mg isotope composition of subduction zone fluids and to reveal the influence of metasomatic processes on Mg isotopes in the subduction channel. Our results suggest that subduction zone fluids derived from carbonated oceanic crust and sediments in the forearc region potentially have Mg isotope compositions lower than oceanic crust or mantle peridotite and thus could create a low $\delta^{26}\text{Mg}$ signature in the mantle.

2. Geological Setting and Samples

Myanmar is located on the eastern prolongation of the Himalayan orogenic system (Figure 1a). From west to east, it comprises the following four major tectonic domains: the Indo-Burma Range, the West Burma Block, the Mogok Belt, and the Shan Plateau (Mitchell et al., 2012; Searle et al., 2007). The Myanmar jadeitite mines are located at the eastern edge of the West Burma Block in a complex association with the Sagaing Fault and the boundary of the Jade Mine Tract with the Nanyaseik Uplift (Mitchell et al., 2007, 2012). The Jade Mine Tract is exposed in the western boundary of the Sagaing Fault in the Hpakan area of Kachin State (Bertrand et al., 1999) and mainly consists of jadeitite-bearing serpentinite mélange, glaucophane schist, mica schist, diopside marble, and amphibolite (Bender, 1983; Shi et al., 2001, 2014). Jadeitite mostly exhibits a white color and occurs as veins (0.5–20 m) or blocks in serpentinitized peridotites or as boulders in drainages and conglomerates in the Jade Mine Tract (Figures 1b, 2a, and 2b). Between the serpentinite and jadeitite veins, there exists a 3–50-cm-wide amphibole-rich blackwall (Figure 2b). Within or along the amphibole-rich blackwall, several green kosmochlor and Cr-jadeite occur as 1–10-cm-wide veins. The country rock of jadeitite is antigorite serpentinite or serpentinitized peridotite (Shi et al., 2012). Rare eclogites and blueschists have been found in the Jade Mine Tract (Goffé et al., 2000; Nyunt, 2009).

The formation age of the Myanmar jadeitite is highly debated. In situ zircon U-Pb data indicate that the formation age of jadeitite is 147–158 Ma (Qiu et al., 2009; Shi et al., 2008, 2009). In contrast, Yui et al. (2013) suggested that such old ages represent inherent protolith ages, with the youngest zircon U-Pb ages, 77 ± 3 Ma, being comparable to the peak metamorphic age. Recently, Eocene $^{40}\text{Ar}/^{39}\text{Ar}$ ages obtained on phengites from quartz schists in the Jade Mine Tract suggested that the jadeitites likely underwent rapid exhumation at ~45 Ma along the Sagaing Fault (Shi et al., 2014).

Most P-type jadeitites occur as veins in serpentinite and have euhedral jadeite crystals with rhythmic zoning under cathodoluminescence and backscattered images, suggesting that they precipitated from

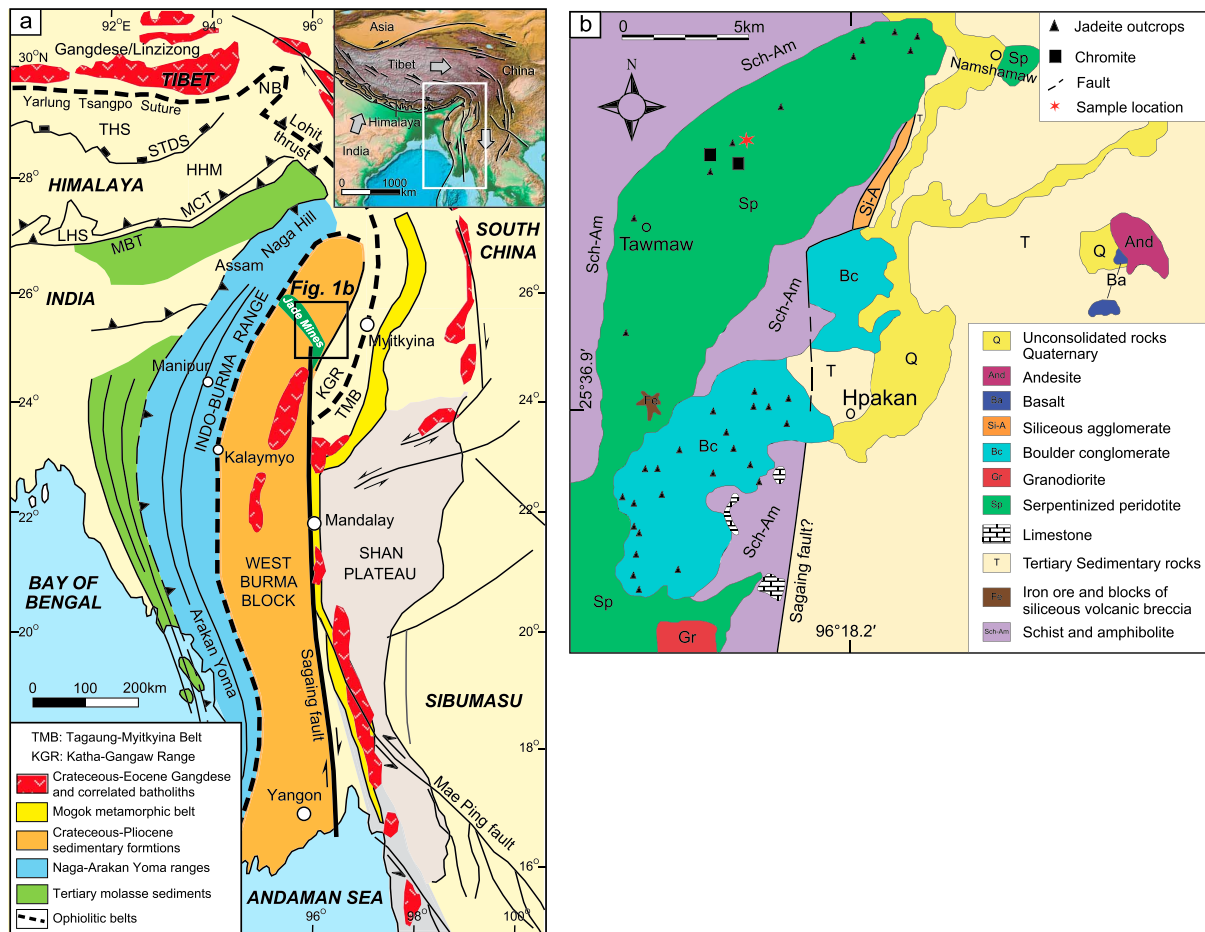


Figure 1. (a) Geological sketch map of Myanmar, modified after Liu et al. (2016). (b) Geological sketch map of the Myanmar jadeite area (modified after Shi et al., 2014).

a Na-Al-Si-rich aqueous fluid (Shi et al., 2008, 2009, 2012; Sorensen et al., 2006). Alternatively, R-type jadeitites preserve textural, mineralogical, or geochemical evidence of a crustal protolith, such as gabbro or plagiogranite (Lei et al., 2016; Ng et al., 2016). The Myanmar jadeitite is enriched in Ba, Pb, Sr, U, and Li and depleted in Rb and K, relative to midocean ridge basalt (Harlow et al., 2015; Shi et al., 2008). The sources of jadeite-forming fluids have previously been interpreted to be subducted altered oceanic crust (AOC), sediments, and/or serpentinites. The highly depleted mantle Hf isotope signatures of zircons in jadeitites suggest that the fluids were derived from the dehydration of altered oceanic mafic crust (Qiu et al., 2009; Shi et al., 2009). However, the presence of Ba-rich minerals, deep-sea spherules, and CH₄-rich fluid inclusions in the Myanmar jadeitites suggests that subducted sediments were also incorporated into the jadeite-forming fluids (Shi et al., 2008, 2010, 2011). In addition, Mg-Cr-rich jadeite rims in jadeitites reflect a minor addition of serpentinite-derived fluid into the jadeite-forming fluids (Sorensen et al., 2006).

The present study focuses on the jadeitites and associated rocks (amphibole-rich blackwall and serpentinite) collected from a natural exposure of the serpentinite mélangé in the Jade Mine Tract (Figures 1b and 2). Generally, the jadeitite samples can be classified into two groups: one group is white jadeitite (Figure 2c), and the other group is green jadeitite (Figure 2d). The white jadeitite primarily consists of jadeite (Figure 3a) with minor accessory omphacite, amphibole, albite, and zircon (Table S1). The jadeite commonly shows rhythmic zoning in Ca and Mg under backscattered images (Figure 3b). The green jadeitite is mainly composed of Cr-bearing jadeite and kosmochlor, with minor omphacite, relict chromite, and sodic amphibole (Figure 3c). The green jadeitite commonly occurs as thin veins (1–10 cm) along the fractures or grain boundaries in the white jadeitite or amphibole-rich zones,

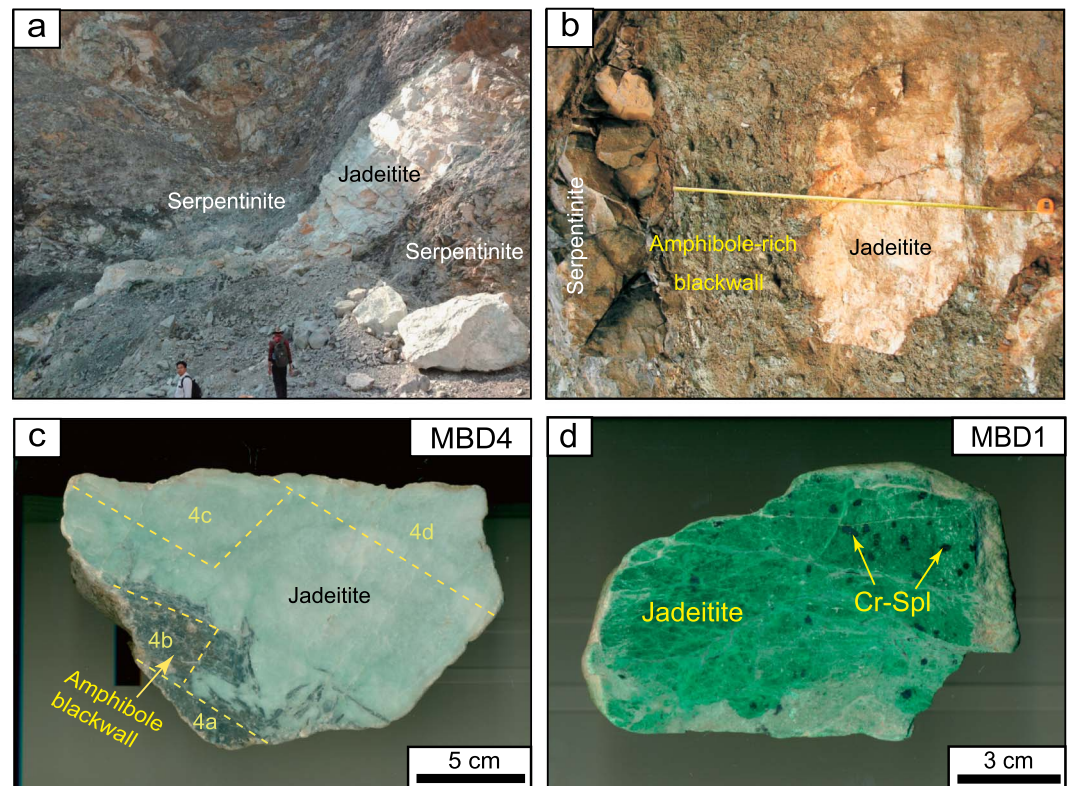


Figure 2. (a) Field photo showing a jadeitite vein in serpentinite from the Hkamti Jade Mine Tract. (b) Amphibole-rich blackwall occurs in the contact boundary between serpentinite and jadeitite (Hkamti, Saging region). The length of band tape is 1 m. (c) White jadeitite with an amphibole-rich boundary. The regions of 4a–4d refer to four samples (MDB4a to MDB4d) that are separated from MDB4. (d) Green jadeitite containing abundant Cr-spinel grains.

implying that the green one is a later-stage metasomatic product (Shi et al., 2012). Several metasomatic textures are observed in the green jadeitite, as characterized by the replacement of chromite by kosmochlor and Cr-bearing jadeite (Figures 3c and 3d). Sodic to sodic-calcic amphiboles occur at the boundaries of the white jadeitites and appear as a blackwall (Figure 3e). Serpentinite can be subdivided into brucite-antigorite (Bru-Atg) serpentinite and olivine-antigorite (Ol-Atg) serpentinite. The Bru-Atg serpentinite (sample A1-1) is mainly composed of brucite and antigorite (Figure 3f), occasionally associated with chlorite, relict Cr-spinel, and clinopyroxene. The Ol-Atg serpentinite (sample J4) adjacent to the jadeitites is characterized by the absence of brucite and the presence of Mg-rich olivine rims with abundant tiny antigorite inclusions (1–3 μm) in direct contact with primary olivine cores (Figures 3g and 3h). A detail description of sample distributions is given in supporting information Text S1. The mineral modal proportions of the studied samples are presented in supporting information Table S1.

3. Methods

3.1. Whole-Rock Major and Trace Elements

Whole-rock major element compositions were analyzed by X-ray fluorescence spectrometry on fused glass disks at the Institute of Geology and Geophysics, Chinese Academy of Sciences. The analytical uncertainties range from 1% to 3% for elements above 1 wt.% and are approximately 10% for elements below 1 wt.%.

Whole-rock trace element concentrations were analyzed by inductively coupled plasma mass spectrometry using a Finnigan Mat Element Spectrometer at the Institute of Geology and Geophysics, Chinese Academy of Sciences. Sample powders were digested in concentrated HF + HNO₃ in high-pressure Savillex Teflon

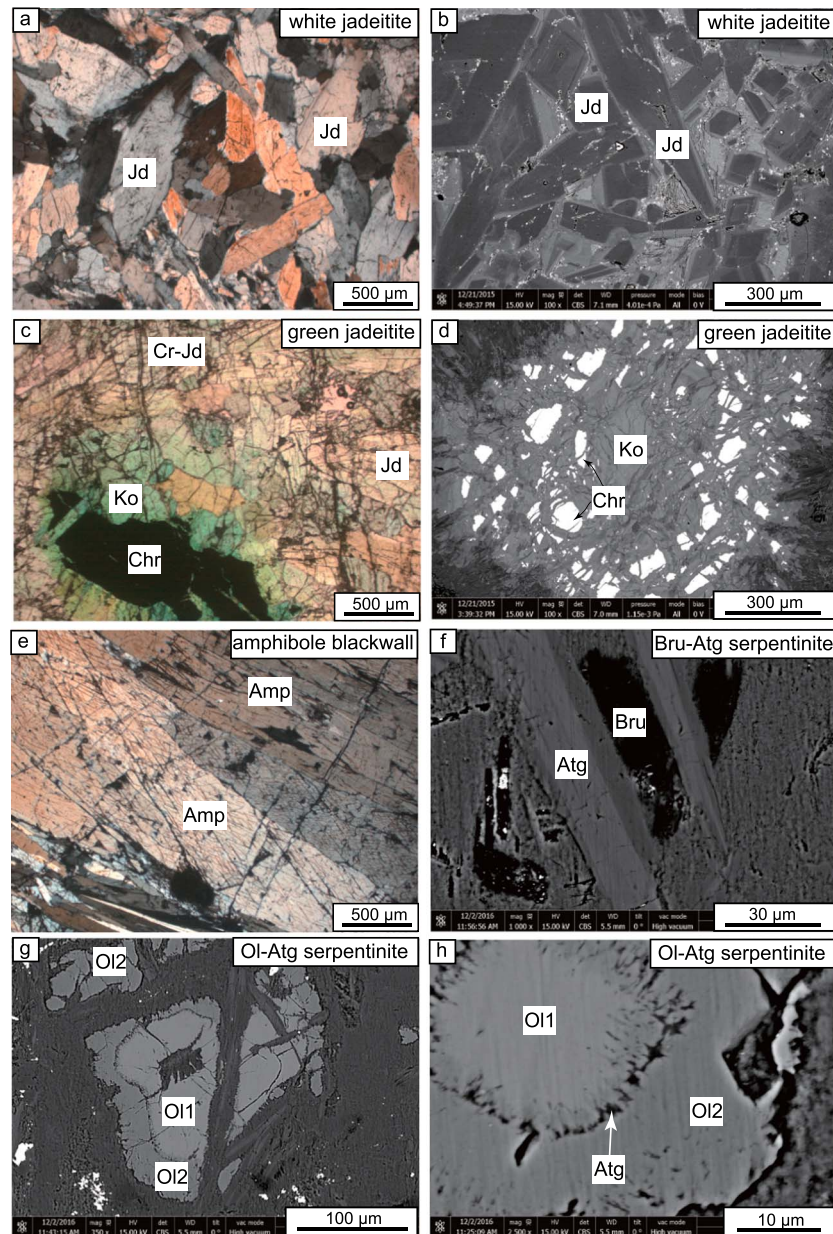


Figure 3. Microphotographs (a, c, d, e) and backscattered electron images (b, f, g, h) showing textures and mineral assemblages in the Myanmar jadeitites and associated rocks. (a) Subhedral jadeite grains in the white jadeitite (MDB5). (b) Rhythmic zoning of jadeite grains in the white jadeitite (MDB4c) is an oscillatory variation in chemical composition. Note that the rims of jadeites show light color due to their high Ca and Mg contents. (c) Replacement of chromite by kosmochlor and Cr-bearing jadeite in the green jadeitite (MDB1). (d) Newly formed kosmochlor cutting chromite into anhedral fragments (MDB1). (e) Coarse-grained amphibole occurring in the boundary of the white jadeitite. (f) Antigorite in contact with brucite in the Bru-Atg serpentinite (A1-1). (g) High-Mg olivine overgrowth rims surrounding the primary olivine in the Ol-Atg serpentinite (J4). (h) Abundant antigorite inclusions occurring in the high-Mg olivine rims. Mineral abbreviations are from Whitney and Evans (2010).

bombs at 120 °C for 7 days, evaporated to near dryness, and then diluted to 50 ml using super-pure HNO₃ for analysis. A blank solution was prepared, and the total procedural blank was <50 ng for all trace elements. Indium was used as an internal standard to correct matrix effects and instrument drift. Two reference standards (GSR-1 and GSR-3) were measured during the course of the analytical procedure. The precision for most trace elements was better than 5%.

Table 1
Magnesium Isotope Composition of Jadeitite, Amphibole Blackwall, and Serpentinite

Sample	Rock type	$\delta^{26}\text{Mg}^a$	2SD	$\delta^{25}\text{Mg}$	2SD	N
MDB-4c	White jadeitite	-1.33	0.08	-0.68	0.04	6
MDB-4d	White jadeitite	-1.24	0.03	-0.62	0.02	3
MDB5	White jadeitite	-1.03	0.06	-0.51	0.04	4
Replicate ^b		-1.03	0.06	-0.53	0.06	4
MDB13	White jadeitite	-1.34	0.04	-0.70	0.02	3
MDB14	White jadeitite	-1.29	0.03	-0.65	0.03	3
MDB16	White jadeitite	-1.55	0.03	-0.79	0.02	3
MDB17	White jadeitite	-0.92	0.02	-0.47	0.01	3
MDB18	White jadeitite	-1.00	0.02	-0.52	0.03	3
Replicate		-0.99	0.01	-0.51	0.03	3
MDB1	Green jadeitite	-0.11	0.04	-0.07	0.04	3
MDB2	Green jadeitite	-0.91	0.06	-0.47	0.02	3
MDB15-1	Green jadeitite	-0.75	0.04	-0.38	0.02	3
MDB15-2	Green jadeitite	-0.74	0.02	-0.37	0.02	3
Replicate		-0.84	0.11	-0.43	0.06	7
J3	Green jadeitite	-0.80	0.01	-0.43	0.05	3
MDB-4a	Amphibole blackwall	-1.16	0.05	-0.60	0.03	6
MDB-4b	Amphibole blackwall	-1.17	0.02	-0.59	0.03	3
MDB3	Amphibole blackwall	-1.08	0.03	-0.55	0.02	3
MDB7	Amphibole blackwall	-0.72	0.02	-0.35	0.02	3
MDB10	Amphibole blackwall	-1.13	0.07	-0.57	0.03	9
J2	Amphibole blackwall	-0.84	0.04	-0.43	0.06	4
J4	Ol-Atg serpentinite	-0.08	0.06	-0.04	0.03	6
A1-1	Bru-Atg serpentinite	-0.26	0.01	-0.13	0.02	3
Standards						
IGG		-1.74	0.06	-0.89	0.04	21
CAM-1		-2.59	0.05	-1.34	0.03	12
GSP-2		0.03	0.05	0.02	0.03	4
BHVO-2		-0.20	0.05	-0.10	0.02	3

^a $\delta^{26}\text{Mg} = ([^{26}\text{Mg}/^{24}\text{Mg}]_{\text{sample}}/[^{26}\text{Mg}/^{24}\text{Mg}]_{\text{DSM3}} - 1) \times 1,000\text{‰}$; DSM3 is solution made from pure Mg metal. ^bReplicate represents repeating sample solution, column chemistry, and instrumental analysis.

3.2. Mineral Major Elements

The major element concentrations of rock-forming minerals were analyzed with a CAMECA SXFive microprobe analyzer at the Institute of Geology and Geophysics, Chinese Academy of Sciences. The analytical conditions are 15-kV accelerating voltage, 20-nA beam current, and 3- μm spot diameter for all minerals. The counting time for most minerals is 20 s on the peak and 10 s on the lower and upper background positions. The counting time for TiO_2 , Al_2O_3 , Cr_2O_3 , MnO , and NiO in olivine is 60 s. The detection limits for these elements are approximately 100–200 ppm. The precision of all major elements was better than 1.5% (3SD).

3.3. Whole-Rock Mg Isotopes

Magnesium isotope ratios were measured using a Thermo Scientific Neptune Plus multicollector-inductively coupled plasma mass spectrometry following the method of An et al. (2014) at the CAS Key Laboratory of Crust-Mantle Materials and Environments at the University of Science and Technology of China, Hefei. Whole-rock powders were digested by a mixture of concentrated HF-HNO_3 . Mg purification was performed in Savillex microcolumns loaded with 2 ml of Bio-Rad AG50W-X12 resin. The blanks were around 5 ng, negligible relative to the amount of purified Mg (20–40 μg). Mg isotope ratios were measured using the sample-standard bracketing method with DSM-3 as the bracketing standard. The Mg isotope results are reported using the standard δ notation relative to DSM-3: $\delta^{26}\text{Mg} (\text{‰}) = ([^{26}\text{Mg}/^{24}\text{Mg}]_{\text{sample}}/[^{26}\text{Mg}/^{24}\text{Mg}]_{\text{DSM-3}} - 1) \times 1,000$. The uncertainties for $\delta^{25}\text{Mg}$ and $\delta^{26}\text{Mg}$ are given as two standard deviations (2SD). Based on the repeated analyses of samples and whole-rock standards, the error for $\delta^{26}\text{Mg}$ is better than 0.06‰ (2SD). The standard data are consistent with literature values within error (Table 1; e.g., An et al., 2014; Huang et al., 2009). Duplicated analyses of rock samples also produced consistent $\delta^{26}\text{Mg}$ data, indicating the reliability of our measurements.

4. Results

4.1. Whole-Rock Compositions

The whole-rock major and trace element contents are presented in supporting information Table S2. The two types of jadeitites have Mg# (= $\text{Mg}/[\text{Mg} + \text{Fe}^{2+}] \times 100$) values of 71–89 and high concentrations of fluid-mobile elements (e.g., Li, Ba, U, Pb, and Sr). The green jadeitites have lower Na_2O (9.39–11.75 wt.%) but higher MgO (4.16–10.40 wt.%) and Cr_2O_3 (0.44–9.54 wt.%) relative to the white ones, which is consistent with their high modal proportions of chromite and kosmochlor observed in thin sections (Figures 2d and 3c). The serpentinite samples have refractory compositions, with high concentrations of MgO (~37 wt.%), Cr (3,830–4,064 ppm), and Ni (1,850–3,358 ppm), and extremely low concentrations of CaO (0.04–0.10 wt.%) and Al_2O_3 (0.32–0.42 wt.%). Compared with the serpentinites, the amphibole-rich blackwalls show lower MgO contents and higher CaO, Na_2O , Al_2O_3 , and SiO_2 contents (Table S2).

4.2. Mineral Chemistry

The detailed compositions of minerals from jadeitites and associated amphibole-rich blackwalls have been investigated in previous studies (e.g., Shi et al., 2003, 2012; Shi, Tropper et al., 2005; Sorensen et al., 2006). Only minerals from serpentinites are summarized in supporting information Table S3. The relict olivine cores (OI1) are characterized by high Mg# (91.6–92.8) and NiO (0.38–0.52 wt.%) contents and low MnO contents (0.11–0.23 wt.%), whereas the secondary olivine rims (OI2) have extremely high Fo values (95.6–97.0) with higher MnO (0.33–0.48 wt.%) and NiO (0.46–0.59 wt.%) contents (Figures 4a and 4b) than OI1. Cr-spinel

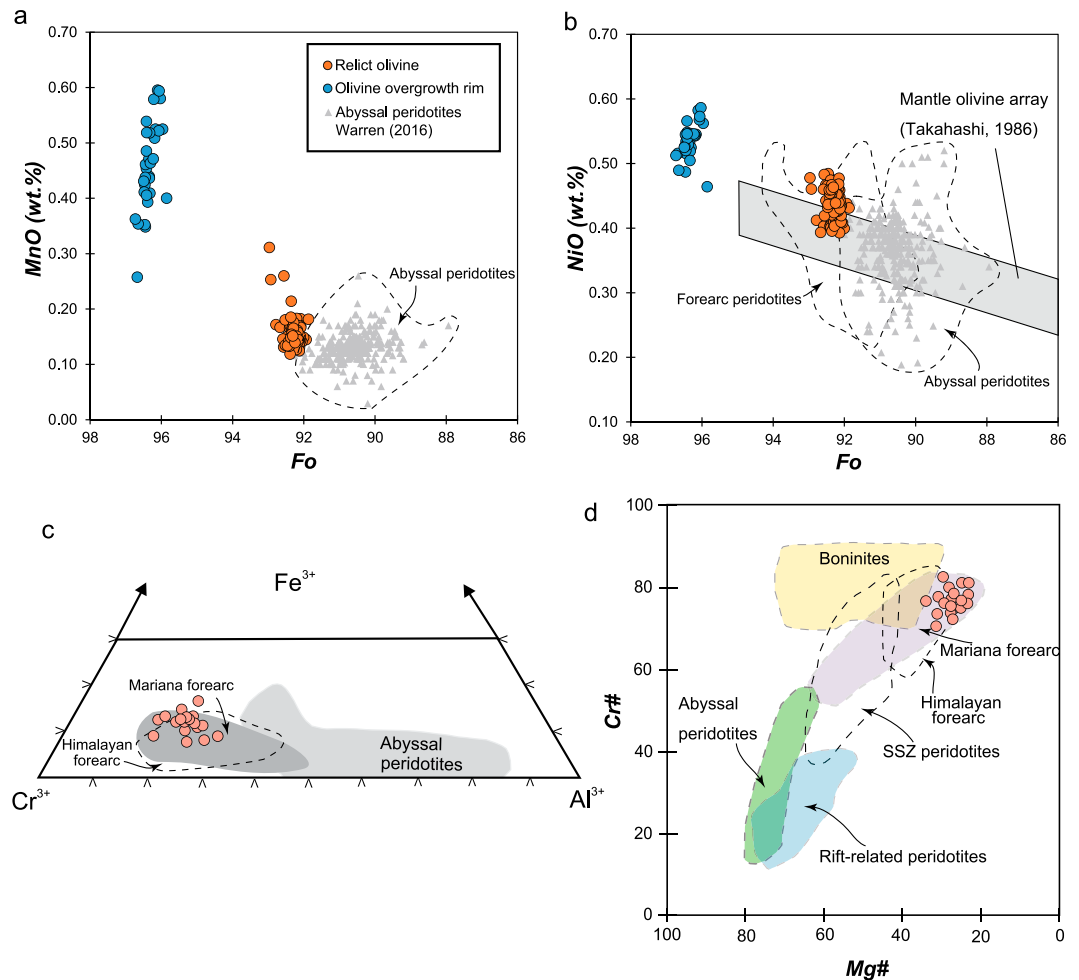


Figure 4. Mineral compositions of olivine and spinel in the serpentinites from the Myanmar Jade Mine Tract. (a) Fo-MnO relations in olivines. (b) Fo-NiO relations in olivines. Olivine mantle array representing the residual mantle olivine (Takahashi, 1986) is shown. The compositions of abyssal peridotites and forearc peridotites are collected from Warren (2016) and Ishii et al. (1992), respectively. (c) Trivalent cation relations of the unaltered cores of chromian spinels. (d) Mg#-Cr# relations in the unaltered cores of chromian spinels. Data sources: The Mariana forearc mantle (Ishii et al., 1992), the Himalayas forearc mantle (Hattori & Guillot, 2007), abyssal peridotites (Barnes & Roeder, 2001; Dick & Bullen, 1984), boninites (Barnes & Roeder, 2001), and rift-related peridotites (Ishwar-Kumar et al., 2016).

grains from both serpentinite samples show systematically higher Cr# (atomic Cr/[Cr + Al] × 100) in the rims due to alteration (e.g., Burkhard, 1993; Kimball, 1990). Homogeneous spinel cores have high Cr# (72–81) and Y_{Fe} ($= Fe^{3+}/[Cr + Al + Fe^{3+}] = 0.12\text{--}0.23$) values and low TiO₂ contents, mostly <0.1 wt.% (Figures 4c and 4d; Table S3). The hydrous minerals have high Mg#, 96–97 for antigorite and 98 for brucite. Antigorite and brucite contain 0.15–0.48 wt.% NiO (Table S3).

4.3. Whole-Rock Mg Isotope Data

The whole-rock Mg isotope data are presented in Table 1. The jadeitites and country rocks display a large range of $\delta^{26}Mg$ values (−1.55‰ to −0.08‰). The Atg-Ol serpentinite has a $\delta^{26}Mg$ value of -0.08 ± 0.06 ‰ (2SD), which is higher than that of the Bru-Atg serpentinite (-0.26 ± 0.01 ‰, 2SD). The two types of jadeitites have distinctively lower $\delta^{26}Mg$ values than the associated serpentinites, with the white jadeitites having values of −1.55‰ to −0.92‰ and the green ones having values of −0.91‰ to −0.74‰ with the exception of sample MDB1, which has an anomalously high $\delta^{26}Mg$ value of −0.11‰. The $\delta^{26}Mg$ values of amphibole-rich zones range from −1.17‰ to −0.72‰, falling between those of the white jadeitites and serpentinites (Figure 5).

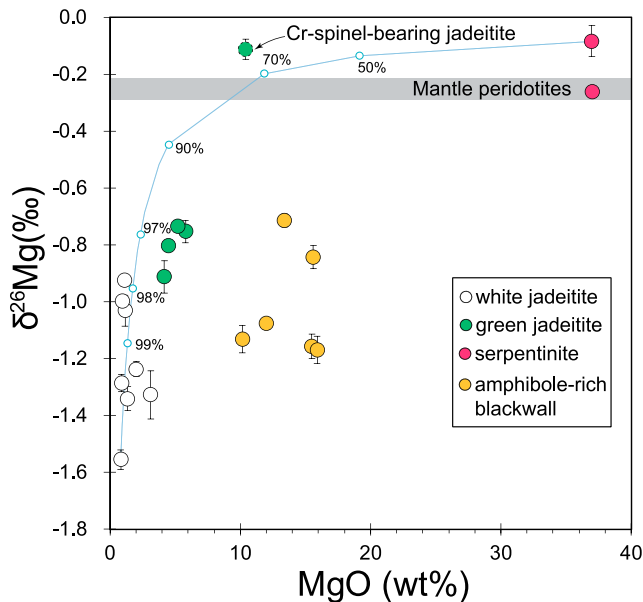


Figure 5. Plots of $\delta^{26}\text{Mg}$ versus MgO for jadeitites and associated rocks from the Myanmar Jade Mine. The Cr-spinel-rich green jadeitites are marked as dashed outline. The shaded area represents the average $\delta^{26}\text{Mg}$ and 2SD of the normal mantle ($-0.25 \pm 0.04\text{‰}$; Teng et al., 2010). Error bars represent 2SD uncertainties. The light blue curve represents binary mixing between white jadeitite and serpentinite. The values along the curve refer to the proportion of white jadeitite.

in Ca and Mg (Figure 3b), suggesting that they were most likely precipitated from Na-Al-Si-rich fluids (Figure 7; Shi et al., 2003, 2012; Sorensen et al., 2006). Such fluids were mainly derived from subducted AOC and sediments (e.g., Harlow et al., 2015; Qiu et al., 2009; Shi et al., 2010, 2011). Minor locally serpentinite-derived fluids might also contribute to the jadeitite-forming fluids (Sorensen et al., 2006); however, no direct mineral evidence for serpentinite dehydration was observed.

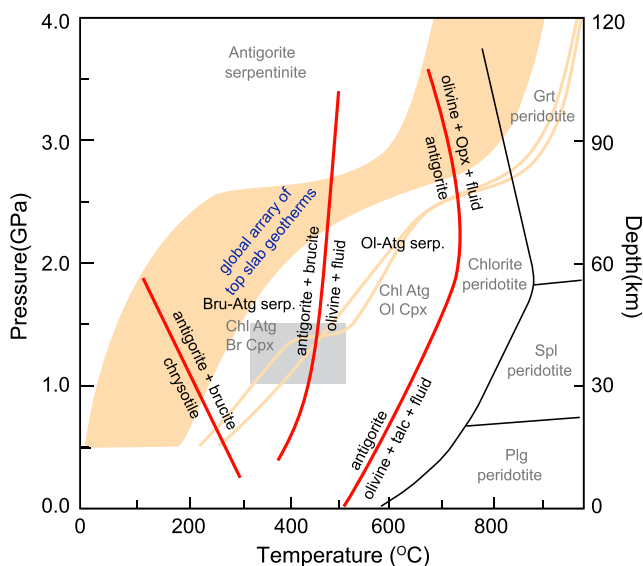


Figure 6. Pressure-temperature diagram illustrating the phase relations and the metamorphic evolution of subducted serpentinites. The P - T paths for the global oceanic subduction interface are from the D80 model of Syracuse et al. (2010). The grey shaded region represents the broad P - T conditions of the Myanmar jadeitites (Shi et al., 2012). The figure is modified from Scambelluri et al. (2004). Mineral abbreviations are from Whitney and Evans (2010).

5. Discussion

5.1. Fluid Sources Along the Subduction Interface

Serpentinites in oceanic subduction zones originate either from the downgoing slab or from the mantle wedge along the subduction interface (Deschamps et al., 2013). Previous studies have proposed that jadeitites may document fluid processes in the forearc mantle (e.g., Harlow et al., 2015, 2016; Tsujimori & Harlow, 2012). Our results further indicate a forearc origin for the host serpentinites. The primary olivine cores from serpentinites have Fo (91.6–92.8), NiO (0.38–0.52 wt.%), and MnO (0.14–0.36 wt.%) values similar to those in refractory mantle peridotites (Tatsumi, 1986) and forearc peridotites (Ishii et al., 1992) but deviate from those in abyssal peridotites (Warren, 2016; Figures 4a and 4b). The composition of Cr spinel is plotted within the forearc mantle field (Figures 4c and 4d) and shows distinctly higher Cr# and lower Mg# values than those observed in abyssal peridotites (Warren, 2016). The consistently high Cr# (76–88) and Y_{Fe} (0.12–0.23) values and low TiO_2 contents (<0.1 wt.%) in the Cr-spinel also reflect the highly refractory nature of the forearc mantle wedge (Arai et al., 2011; Pearce et al., 2000). In addition, the P - T conditions of the Myanmar jadeitites, 1.0–1.5 GPa and 300–500 °C (Shi et al., 2012), are similar to those along the subduction interface at forearc depths (Figure 6; Penniston-Dorland et al., 2015). Therefore, the jadeitites likely formed at the forearc slab-mantle interface.

The jadeitites in the white jadeitites commonly exhibit rhythmic zoning in Ca and Mg (Figure 3b), suggesting that they were most likely precipitated from Na-Al-Si-rich fluids (Figure 7; Shi et al., 2003, 2012; Sorensen et al., 2006). Such fluids were mainly derived from subducted AOC and sediments (e.g., Harlow et al., 2015; Qiu et al., 2009; Shi et al., 2010, 2011). Minor locally serpentinite-derived fluids might also contribute to the jadeitite-forming fluids (Sorensen et al., 2006); however, no direct mineral evidence for serpentinite dehydration was observed.

The Ol-Atg serpentinite surrounding the Myanmar jadeitites preserves mineral textural and compositional evidence for serpentinite dehydration. The secondary olivines in the Ol-Atg serpentinite, characterized by overgrowth rims surrounding the primary olivines, commonly include tiny antigorite (Figures 3g and 3h). This texture and the wide chemical variation of olivine (Figure 4a) are characteristics of deserpentinization in subduction-zone peridotites (Arai et al., 2012; Nozaka, 2003; Yang & Powell, 2008). The secondary olivine rims contain high MgO (Fo_{96-97}), clearly greater than the normal mantle olivine ($<\text{Fo}_{95}$; Arai, 1982), suggesting that the olivine likely formed by the dehydration of brucite or antigorite. Their high NiO contents (up to 0.6 wt.%) most likely result from brucite or antigorite with high NiO contents (0.23–0.48 and 0.15–0.31 wt.%, respectively) during deserpentinization.

The subducting slab can release aqueous fluids that infiltrate the overlying mantle wedge, forming a serpentinite layer at the forearc slab-mantle interface (Bebout & Penniston-Dorland, 2016; Deschamps et al., 2013; Guillot et al., 2009). During the further subduction of serpentinite at the interface, fluids are progressively released by the prograde dehydration of chrysotile/lizardite, brucite, antigorite, and chlorite (Figure 6). The Bru-Atg serpentinite may be produced at the shallow slab-mantle interface (300–450 °C). The absence of brucite and orthopyroxene, as well as the occurrence of secondary high-Mg

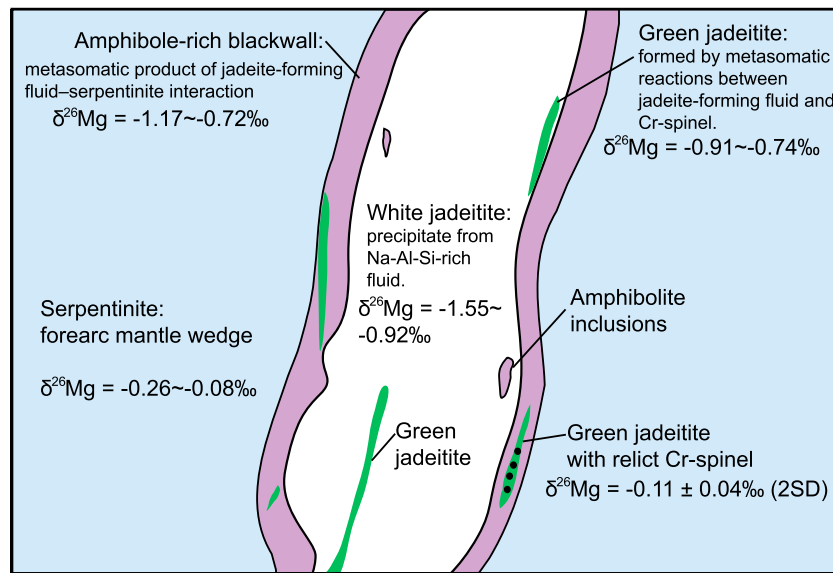
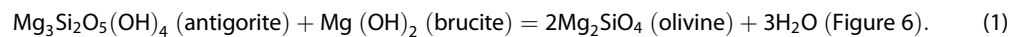


Figure 7. Cartoon illustrating the distribution and Mg isotope compositions of jadeitites, amphibole blackwall, and serpentinite.

olivine in the Ol-Atg serpentinite, implies that brucite is dehydrated out via the following reaction (Ulmer & Trommsdorff, 1995):



This reaction commonly occurs in the forearc region (450–650 °C) and releases Cl-rich fluids (Scambelluri et al., 2004; Scambelluri & Tonarini, 2012; Sharp & Barnes, 2004). This is consistent with the high-salinity aqueous fluid inclusions observed in the Myanmar jadeitites (Qi et al., 2015). Consequently, the jadeite-forming fluids are sourced from not only AOC and sediments but also serpentinite. Such fluids with multiple sources are very common at the slab-mantle interface (e.g., Bebout & Penniston-Dorland, 2016; Manning, 2004; Marschall & Schumacher, 2012).

5.2. Mg Isotope Constraints on the Origin of Jadeite-Forming Fluids

Mg isotopes are not significantly fractionated during melting and crystallization (Liu et al., 2010; Teng et al., 2010, 2016). Metamorphic dehydration only generates limited Mg isotope fractionation (<0.07‰) on a bulk-rock scale (Li et al., 2011; Li, Teng, et al., 2014; Wang et al., 2014). Recent studies have demonstrated that the Mg isotope signatures of subduction zone fluids are likely inherited from Mg-rich hydrous minerals in source reservoirs (Chen et al., 2016; Wang et al., 2017). Given the limited isotopic fractionation, Mg isotopes can be used to provide further constraints on the source composition of jadeite-forming fluids.

Both the Myanmar jadeitites (−1.55‰ to −0.74‰) and amphibole-rich blackwalls (−1.17‰ to −0.72‰) show significantly lower $\delta^{26}\text{Mg}$ than the normal mantle values (−0.25 ± 0.04‰; Teng et al., 2010; Figures 5 and 8). Such low values are first going to be considered in terms of diffusion.

The depleted ^{26}Mg in the jadeitites could be due to a kinetic effect such as thermal or chemical diffusion (Huang et al., 2010; Pogge von Strandmann et al., 2015; Richter et al., 2003). As experimental studies show, diffusion along a thermal or chemical potential gradient can be accompanied by significant isotopic fractionation (Huang et al., 2010; Richter et al., 2003). Because of the lack of melt during the formation of jadeitites at low temperatures (<500 °C; Goffé et al., 2000; Harlow et al., 2015; Shi et al., 2003, 2012), thermal diffusion is considered to be too sluggish to play an important role (Huang et al., 2009). Chemical diffusion by Mg-rich fluids can also induce significant Mg isotope fractionation (Pogge von Strandmann et al., 2011, 2015). If Mg diffusion occurs along the serpentinite-jadeitite interface, the markedly low $\delta^{26}\text{Mg}$ values in the jadeitites and amphibole-rich blackwalls would primarily originate from metasomatic fluids. Regardless of the

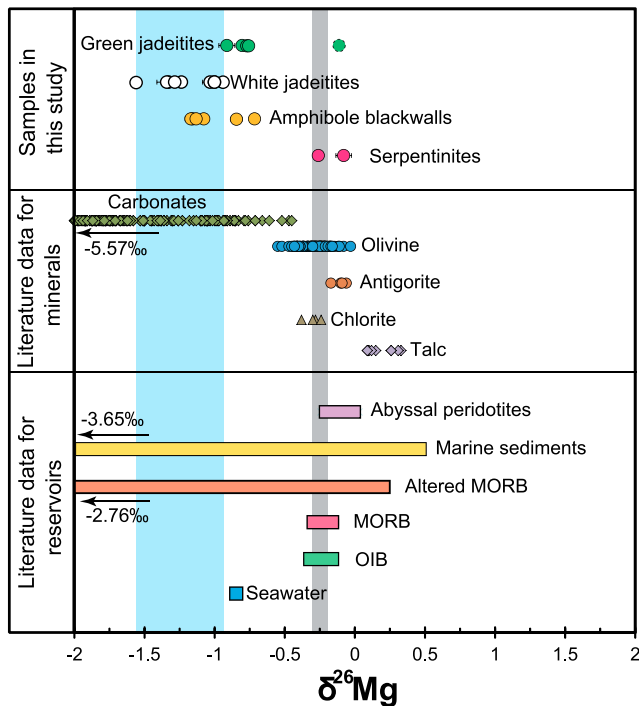


Figure 8. Magnesium isotope composition of the studied samples compared to subduction zone reservoirs and minerals. The gray shaded area represents the mantle $\delta^{26}\text{Mg}$ values after Teng et al. (2010). The blue shaded area represents the $\delta^{26}\text{Mg}$ values of white jadeitites. Data sources: Seawater (Ling et al., 2011); oceanic island basalt (OIB), and midocean ridge basalt (MORB; Bourdon et al., 2010; Teng et al., 2010); altered MORB (Huang, 2013; Huang, Ke et al., 2015; Teng et al., 2016); marine sediments (Hu et al., 2017; Teng et al., 2016); abyssal peridotite (Liu et al., 2017); talc and antigorite (Beinlich et al., 2014); chlorite (Pogge von Strandmann et al., 2015); olivine (Handler et al., 2009; Yang et al., 2009; Young et al., 2009; Huang et al., 2011; Liu et al., 2011; Pogge von Strandmann et al., 2011; Xiao et al., 2013); carbonates (Brenot et al., 2008; Fantle & Higgins, 2014; Geske et al., 2014; Higgins & Schrag, 2010; Hippler et al., 2009; Huang & Xiao, 2016; Jacobson et al., 2010; Kasemann et al., 2014; Tipper et al., 2006; Wombacher et al., 2011).

conditions of chemical diffusion, a negative correlation between MgO and $\delta^{26}\text{Mg}$ should be expected (Pogge von Strandmann et al., 2015). However, this is not the case in the white jadeitites and amphibole-rich blackwalls observed in this study (Figure 5). Therefore, both thermal and chemical diffusion are unlikely to create the low $\delta^{26}\text{Mg}$ signatures in the white jadeitites. Given that the white jadeitites directly precipitated from aqueous fluids (Figure 7), the low $\delta^{26}\text{Mg}$ in the white jadeitites is better explained by low $\delta^{26}\text{Mg}$ sources.

Compared to mantle peridotites, subducted abyssal peridotites have slightly higher $\delta^{26}\text{Mg}$ values of -0.25‰ to $+0.10\text{‰}$ (Figure 8), likely attributed to the formation of secondary Fe oxides and clays (Liu et al., 2017). One explanation for the low $\delta^{26}\text{Mg}$ in the fluids is the breakdown of brucite, as observed in the Ol-Atg serpentinite. Because brucite cannot be physically separated from our samples (Figure 3f), we cannot directly analyze the Mg isotope composition of brucite. However, brucite formation experiments indicate that brucite preferentially takes up higher $\delta^{26}\text{Mg}$ than aqueous fluid (Wimpenny et al., 2014) or does not fractionate Mg isotopes at temperatures of $>40^\circ\text{C}$ (Li, Beard, et al., 2014). In addition, theoretical calculations suggest that Mg isotope fractionation between olivine and aqueous fluid is $<0.2\text{‰}$, even at temperatures as low as 300°C (Schauble, 2011). Although the Mg isotope composition of metamorphic olivine ($\text{Fo} > 96$) has not yet been reported, it is speculated to be not significantly different from the normal mantle olivine (-0.26 ± 0.18 , 2SD, $n = 108$; Figure 8), because olivines contain the same 6-coordinated Mg and Mg-O bonding environment. In this regard, the brucite breakdown fluid equilibrated with the newly formed olivine is unlikely to have $\delta^{26}\text{Mg}$ values as low as -1.55‰ , especially at temperatures of $>450^\circ\text{C}$ (Figure 6). Although chlorite in serpentinite has $\delta^{26}\text{Mg}$ values (-0.38‰ to -0.24‰) slightly lower than mantle peridotites (Pogge von Strandmann et al., 2015), it would be stable at the jadeite-forming conditions (Figure 6) and therefore cannot be the primary source for low $\delta^{26}\text{Mg}$ fluids. Other Mg-rich hydrous minerals, such as antigorite and talc, have high $\delta^{26}\text{Mg}$ values (Figure 8; Beinlich et al., 2014), which also could not release low $\delta^{26}\text{Mg}$ fluids. Therefore, the dehydration of serpentinite alone cannot result in fluids with significantly low $\delta^{26}\text{Mg}$ values.

Subducted AOC and sediments have highly variable $\delta^{26}\text{Mg}$ values from -3.65‰ to $+0.52\text{‰}$ (Figure 8), with low $\delta^{26}\text{Mg}$ in carbonated rocks and with high $\delta^{26}\text{Mg}$ in carbonate-free rocks (Hu et al., 2017; Huang, 2013; Huang, Ke et al., 2015; Teng, 2017; Teng et al., 2016). Therefore, carbonate-rich AOC and sediments are potential sources for the low $\delta^{26}\text{Mg}$ fluids. Carbonates in subducted sediments and AOC commonly have high concentrations of Ca and Sr and high CaO/TiO_2 and $\text{CaO}/\text{Al}_2\text{O}_3$ ratios (Huang & Xiao, 2016; Wang et al., 2015). The $\delta^{26}\text{Mg}$ values of white jadeitites are negatively correlated with CaO/TiO_2 , $\text{CaO}/\text{Al}_2\text{O}_3$, and Sr (Figure 9), implying that recycled carbonates are incorporated into the jadeite-forming fluids. This is also supported by CH_4 -rich fluid inclusions observed in the white jadeitites (Qi et al., 2015; Shi, Tropper et al., 2005), which were likely derived from carbonate-rich source (e.g., carbonate-rich marine sediments or AOC). In addition, diopside marbles do occur in the Jade Mine Tract (Bender, 1983; Shi et al., 2001) and thus potentially provide a carbonate source for the jadeite-forming fluids. $\text{MgO}/\text{Al}_2\text{O}_3$ is not clearly correlated with $\delta^{26}\text{Mg}$ values, suggesting that the incorporated carbonate is likely calcite (Figure 9b). In the following sections, we will focus on the process of how Mg isotopes behave during carbonate recycling in the forearc region.

5.3. Low $\delta^{26}\text{Mg}$ Fluids: The Role of Carbonate Dissolution

Carbon transfer in subduction zone fluids is induced by decarbonation or dissolution processes (Ague & Nicolescu, 2014; Gorman et al., 2006; Kelemen & Manning, 2015; Kerrick & Connolly, 1998, 2001). However,

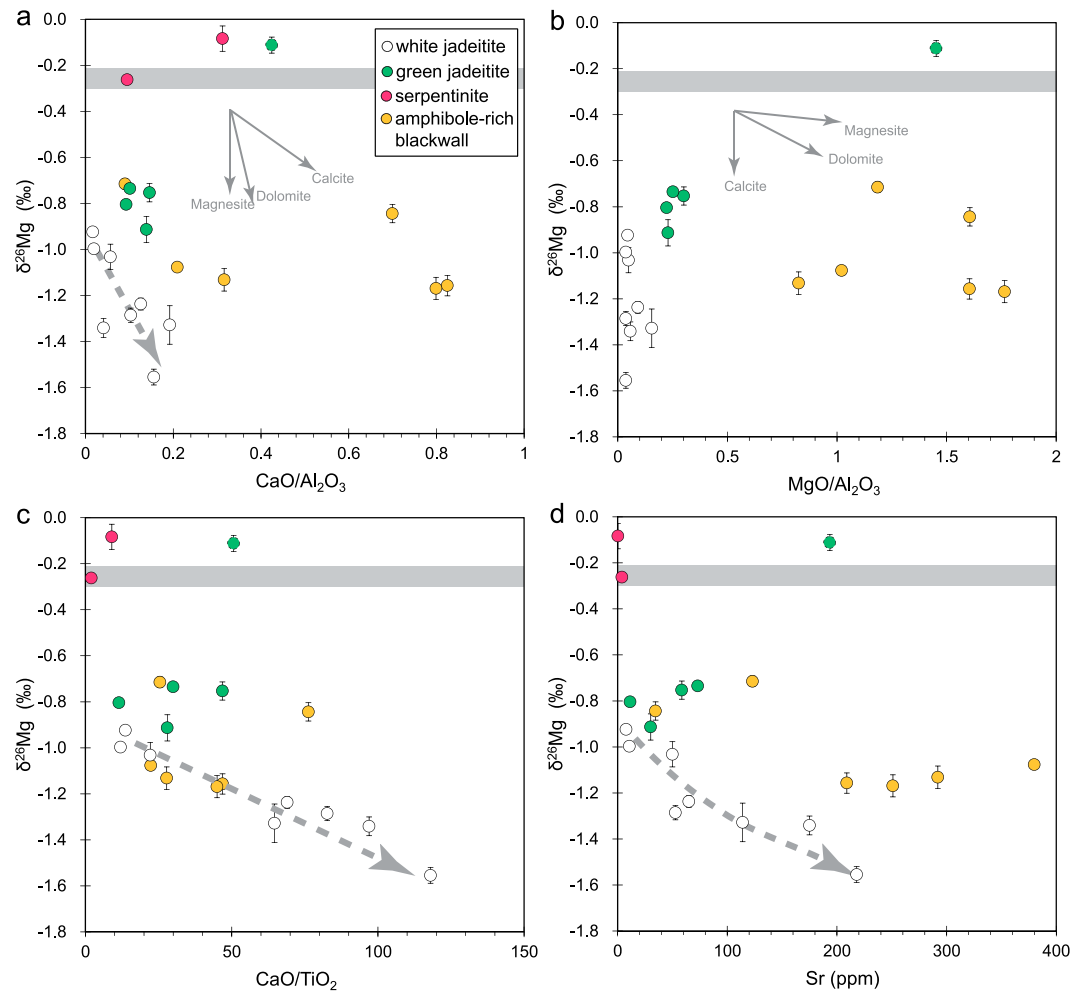


Figure 9. Correlation between whole-rock $\delta^{26}\text{Mg}$ values and $\text{CaO}/\text{Al}_2\text{O}_3$ (a), $\text{MgO}/\text{Al}_2\text{O}_3$ (b), CaO/TiO_2 (c), and Sr (d) values for jadeitites and country rocks from Myanmar. The shaded area represents the mantle $\delta^{26}\text{Mg}$ values after Teng et al. (2010).

carbonates can remain stable to very high pressures and temperatures in subduction zones, resulting in inefficient decarbonation in forearcs (Collins et al., 2015; Dasgupta & Hirschmann, 2010; Kerrick & Connolly, 2001; Molina & Poli, 2000; Poli et al., 2009; Thomsen & Schmidt, 2008). Furthermore, the formation temperatures of the Myanmar jadeitites ($T < 500^\circ\text{C}$) are significantly lower than the decarbonation conditions (Goffé et al., 2000; Shi et al., 2003, 2012). This leaves carbonate dissolution as the best explanation for the incorporation of recycled carbonate into the jadeite-forming fluids.

Theoretical modeling and experimental work demonstrate that aqueous fluids released from oceanic crust and serpentinite at forearc conditions ($< 600^\circ\text{C}$ and $< 2.2\text{ GPa}$) have low MgO contents ($< 0.1\text{ wt.}\%$; Galvez et al., 2015; Manning, 2004; Schneider & Egger, 1986). Aqueous fluids derived from sediments also have extremely low Mg concentrations ($< 200\text{ ppm}$), even at 650°C and 2.2 GPa (Spandler et al., 2007). This is clearly supported by the composition of white jadeitites. The white jadeitites precipitated from Na-Al-Si fluids have $0.84\text{--}3.13\text{ wt.}\%$ MgO (Table S2). According to the jadeitite formation conditions ($1\text{--}1.5\text{ GPa}$, $300\text{--}500^\circ\text{C}$) and experimental work on Na-Al-Si-rich fluids (Manning et al., 2010; Wohlers et al., 2011), the bulk solubility in Na-Al-Si-rich fluid is significantly lower than $3.4\text{ wt.}\%$. Therefore, if all MgO in the fluids was incorporated into the jadeitites during crystallization, the Na-Al-Si fluids would have MgO contents lower than $0.03\text{--}0.10\text{ wt.}\%$. Conversely, carbonate species dissolved in subduction zone fluids are mainly calcite/aragonite (Ague & Nicolescu, 2014; Kelemen & Manning, 2015; Pan et al., 2013), which could have $0.8\text{--}2.0\text{ wt.}\%$ MgO (Huang & Xiao, 2016; Liu et al., 2015). Mg-calcite/aragonite commonly has very low $\delta^{26}\text{Mg}$ signature, with $\delta^{26}\text{Mg}$

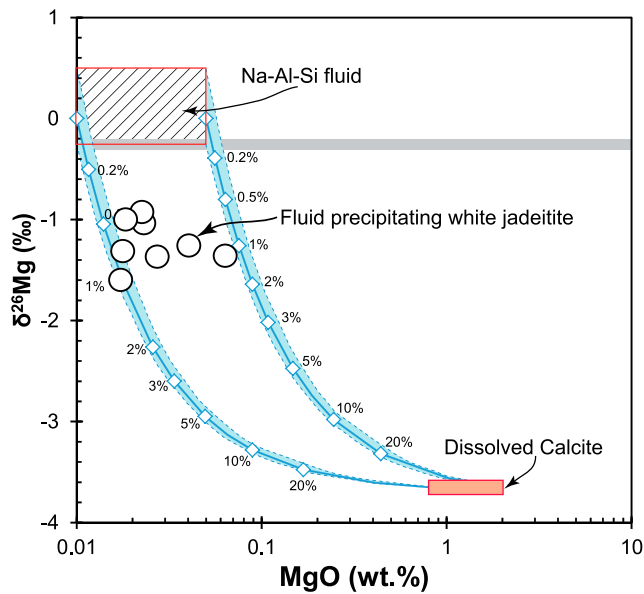


Figure 10. Binary mixing model calculations compared to the MgO and Mg isotopic data from the white jadeitites. The blue lines are mixing trends between Na-Al-Si fluid and calcite/aronite. The compositional range of jadeite with rhythmic zoning (Shi et al., 2003, 2012) is used to represent the anhydrous composition of the initial Na-Al-Si fluid, which is derived from subducted altered oceanic crust and sediments, with minor addition of fluid released by serpentinite. We assume that the bulk solubility of Na-Al-Si fluid is 2 wt.%, based on the experimental data (1 GPa, 500 °C) of Manning et al. (2010) and Wohlers et al. (2011). The MgO values of the Na-Al-Si fluid and those precipitating white jadeitites are recalculated on the basis of this bulk solubility value. The $\delta^{26}\text{Mg}$ of the Na-Al-Si fluid is assumed to be -0.25‰ to $+0.5\text{‰}$, because fluids released from Mg-rich hydrous minerals (e.g., mica and serpentine) may have high $\delta^{26}\text{Mg}$ values. Note that the change of this value will not affect the modeling significantly, as the Na-Al-Si fluid contains too little Mg. The MgO (0.8–2.0 wt.%) and $\delta^{26}\text{Mg}$ (-3.65‰) values of calcite/aronite are taken from Liu et al. (2015) and Huang and Xiao (2016). Numbers at diamond symbols represent the fraction of dissolved calcite/aronite.

ranging from -5.57‰ to -1.04‰ and an average value of $-3.65 \pm 2.17\text{‰}$ ($n = 284$, 2SD, Huang & Xiao, 2016). Therefore, the Mg isotope composition of aqueous fluids released at forearc depths can be easily modified by dissolved calcite/aronite. The Mg isotope composition of Na-Al-Si-rich fluid is unknown; however, most clays and other hydrous minerals in subducting reservoirs appear to have $\delta^{26}\text{Mg}$ values higher than mantle peridotites (Beinlich et al., 2014; Liu et al., 2017; Teng, 2017; Wang et al., 2017). Here we assume a broad range of $\delta^{26}\text{Mg}$ values (-0.25‰ to $+0.5\text{‰}$), which will not affect the modeling significantly because of the low MgO content in the Na-Al-Si-rich fluid. Our modeling results show that the low $\delta^{26}\text{Mg}$ values in the white jadeitites only require adding 0.5–1% of Mg-calcite/aronite with $\delta^{26}\text{Mg} = -3.65\text{‰}$ and 0.8–2.0 wt% MgO (Huang & Xiao, 2016; Liu et al., 2015) to the Na-Al-Si-rich fluid (Figure 10).

Experimental studies show that the solubility of calcite/aronite in aqueous fluid may be considerable at forearc P - T conditions (e.g., Caciagli & Manning, 2003; Manning et al., 2013; Pan et al., 2013). In addition, the solubility of carbonates increases at a given P - T condition with decreasing pH (Manning, 2013), with addition of NaCl (Newton & Manning, 2002), and decreasing oxygen fugacity (Lazar et al., 2014). Both high-salinity and CH_4 -rich, reduced aqueous fluid inclusions have been observed in the Myanmar jadeite (Qi et al., 2015; Shi, Tropper et al., 2005), which are likely to enhance the solubility of Ca-rich carbonate in the jadeite-forming fluids.

5.4. Effects of Metasomatism on Mg Isotopes

The results of this study can further constrain the effects of metasomatism on the Mg isotope composition of jadeitites and amphibole-rich blackwalls. The amphibole-rich blackwall, as a spatial and chemical intermediate between jadeite and serpentinite, is commonly considered to be the metasomatic product of the jadeite-forming fluid-serpentinite interaction (Figure 7; Shi et al., 2003, 2012). The MgO contents and $\delta^{26}\text{Mg}$ values of amphibole-rich blackwalls fall between jadeite and serpentinite (Figure 5), further indicating that the jadeite-forming fluids have low $\delta^{26}\text{Mg}$. However, the white jadeite-serpentinite mixing curve clearly does not fit the data measured on the amphibole-rich blackwalls (Figure 5). This suggests that the amphibole-rich blackwall formed in an open-system process with high fluid/rock ratios.

process with high fluid/rock ratios.

The green jadeitites formed by metasomatic reactions between jadeite-forming fluids and Cr-spinel (Figure 7; Mével & Kiéna, 1986; Shi, Stöckhert et al., 2005; Shi et al., 2012). The green jadeitites show large variations in $\delta^{26}\text{Mg}$ (Figure 5), with the highest value ($-0.11 \pm 0.04\text{‰}$) recorded in the sample MDB1 (Table 1). Spinel commonly has higher $\delta^{26}\text{Mg}$ values (0.41–0.66‰) than coexisting olivine and pyroxene (Young et al., 2009). The high $\delta^{26}\text{Mg}$ for green jadeite MDB1 may be simply due to the overabundance of Cr spinel, as supported by the high concentrations of Cr_2O_3 (9.54 wt.%) and Fe_2O_3 (6.05 wt.%; Table S2). However, the other four green jadeitites (MDB2, J3, MDB15-1, and MDB15-2), which are almost free of Cr-spinel, still exhibit higher $\delta^{26}\text{Mg}$ values than the white group (Figure 5). Compared with the white jadeitites, the green jadeitites have additional kosmochlor and diopside components in Cr-rich clinopyroxene (Table S1). The metasomatic texture preserved in MDB1 suggests that the Cr-rich clinopyroxene formed by the replacement of Cr spinel (Figure 11a). X-ray mapping shows that the Cr-spinel preserves compositional zoning characterized by an outward increase in Fe but decrease in Mg (Figures 11b and 11c). This indicates that Mg is lost from the Cr spinel into the newly formed Cr-rich clinopyroxene. The loss of isotopically heavy Mg during this metasomatic process may increase the $\delta^{26}\text{Mg}$ of the green jadeitites, which is in good agreement with our results (Figure 11d). Previous petrological studies indicated that the breakdown of Cr spinel was a late-stage process, as recorded by Cr-rich clinopyroxene (green jadeitites) via late-stage veining along the fractures of the white jadeitites at centimeter to decimeter scales (Harlow et al., 2015; Shi, Stöckhert et al., 2005; Shi et al., 2012).

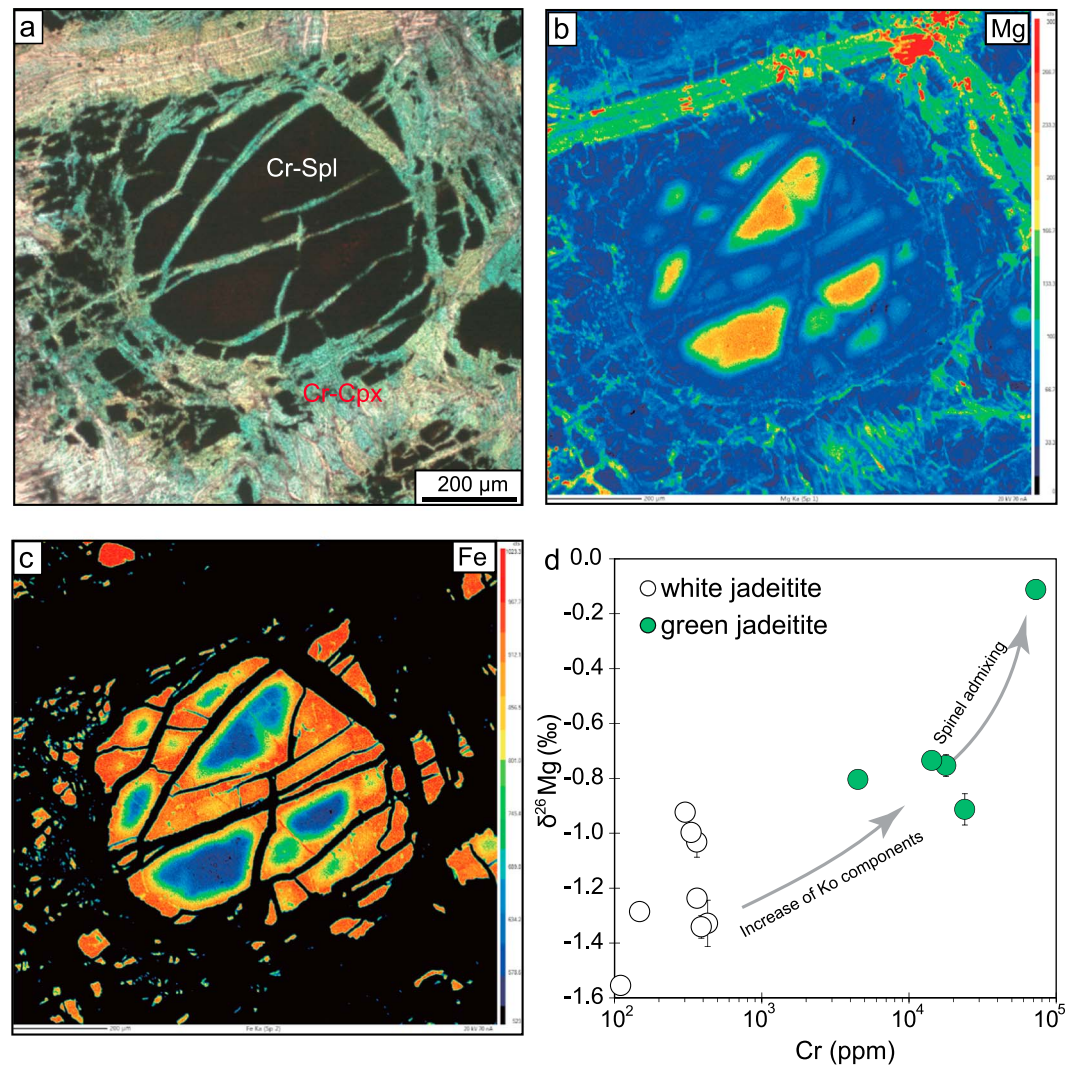


Figure 11. (a) Microphotograph and X-ray maps (b, c) showing the replacement texture of chromite by Cr-rich clinopyroxene (kosmochlor) in sample MDB1. Note the outward increase of Fe but decrease of Mg in the chromite interior. (d) Correlation between $\delta^{26}\text{Mg}$ and Cr for the two types of jadeitites.

Thus, various degrees of interaction between the jadeite-forming fluids and serpentinite/Cr-spinel could generate a large $\delta^{26}\text{Mg}$ range in the green jadeitites and amphibole-rich blackwalls, inducing large Mg isotope heterogeneity in a localized area along the subduction interface.

5.5. Implications for Tracing Carbon Cycling in Forearc Regions Using Mg Isotopes

Deep carbon recycling is an important process for carbon budgets in terrestrial reservoirs (e.g., Dasgupta & Hirschmann, 2010; Kelemen & Manning, 2015). Recent studies show that Mg isotopes play a powerful tracer for recycled carbonates in the deep mantle (Huang, Li et al., 2015; Li et al., 2017; Tian et al., 2016; Yang et al., 2012). For example, the low Mg isotope compositions of some intraplate basalts have been attributed to the interaction of mantle peridotite with carbonatitic melts derived from subducted oceanic slab in the mantle transition zone (Huang, Li et al., 2015; Li et al., 2017; Yang et al., 2012). However, carbonates are unlikely to dominate the Mg budget at subarc depths (80–150 km), as some arc lavas have slightly higher $\delta^{26}\text{Mg}$ values relative to the normal mantle (Li et al., 2017; Teng et al., 2016). This indicates that subduction zone fluids at subarc depths are likely to have high $\delta^{26}\text{Mg}$ values, which are possibly inherited from Mg-rich hydrous minerals with high $\delta^{26}\text{Mg}$ (Chen et al., 2016; Wang et al., 2017). In addition, dehydrated fluids at subarc depths could have considerable MgO (Dvir et al., 2011; Kessel et al., 2005; Spandler et al., 2007). Therefore,

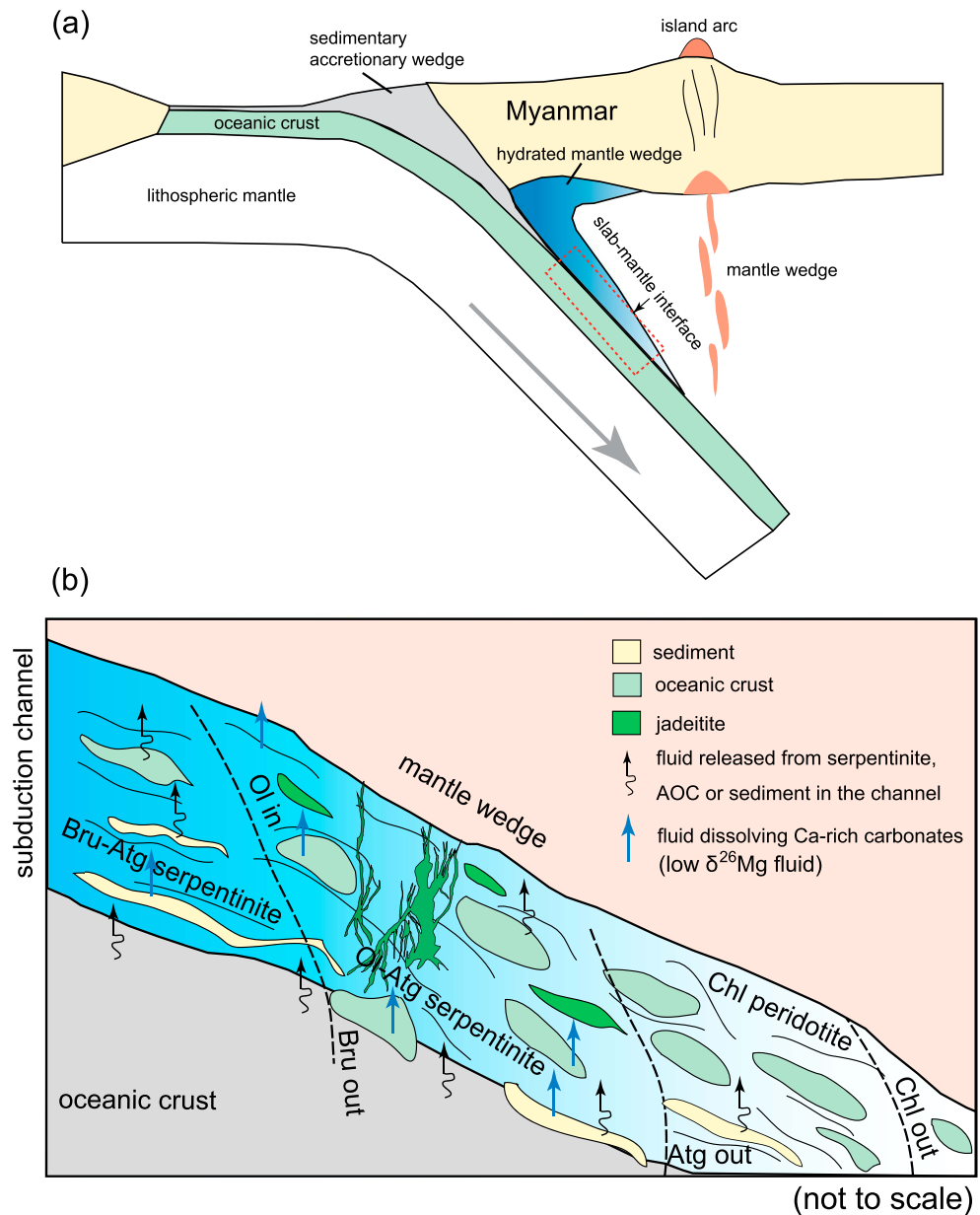


Figure 12. Schematic diagrams (not to scale) illustrating the possible geodynamic scenarios for the formation of jadeitites from Myanmar. (a) Typical oceanic subduction system, with the hydrated mantle wedge, the plate interface, and the downgoing slab distinguished with different colors. (b) Larger-scale diagram showing fluid activities in the serpentinized subduction channel such as the Myanmar jadeite area. At the early stage, the mantle wedge was hydrated by fluids derived from the dehydration of the subducting hydrated slab, and a subduction channel was formed at the slab-mantle interface. Large amounts of serpentine minerals, brucite, and chlorite were formed at this stage. Prograde metamorphism by the downgoing altered oceanic crust (AOC) and sediments would release Na-Al-Si-rich fluids. Such fluids dissolve Ca-rich carbonates along migration conduits and precipitate white jadeite veins or blocks with systematically low $\delta^{26}\text{Mg}$. Locally, the jadeite-forming fluid reacted with the surrounding serpentinite (or chromite) to form higher $\delta^{26}\text{Mg}$, heterogeneous amphibole blackwall, and green jadeite, which were then exhumed to the surface.

dissolved Ca-rich carbonates may have a limited influence on the Mg isotope composition of subduction zone fluids at subarc depths.

The Mg isotope composition of subduction zone fluids at forearc depths (<80 km) may be different from those at subarc depths. Because Mg solubility in aqueous fluids strongly increases with pressure and temperature (Manning, 2004; Stalder et al., 2001), dehydrated fluids in forearc regions have very low MgO

concentrations (Galvez et al., 2015; Manning, 2004; Spandler et al., 2007). A small fraction of Ca-rich carbonate (e.g., Mg-calcite) dissolution would significantly decrease the $\delta^{26}\text{Mg}$ values of aqueous fluids, as shown in Figure 10. Experimental studies and observations for carbonated hydrothermal veins and CH_4 -rich fluid inclusions in natural high-pressure rocks indicate that significant carbon could be released from slabs at forearc depths via carbonate dissolution (Ague & Nicolescu, 2014; Caciagli & Manning, 2003; Kelemen & Manning, 2015; Scambelluri et al., 2015, 2016; Song et al., 2009). The jadeitite in the forearc region has captured a snapshot of dissolved carbonates in subduction zones (Figure 12). Thus, considering the common occurrence of Ca-rich carbonates in sediments and AOC (Alt & Teagle, 1999), shallow subduction zone fluids that dissolve carbonates are likely to have low $\delta^{26}\text{Mg}$.

Aqueous fluid may be transferred in the slab-mantle interface through a channelized conduit (Bebout & Penniston-Dorland, 2016; John et al., 2008; Plümpner et al., 2017); thus, open-system metasomatism with high fluid/rock ratios may be archived. The low $\delta^{26}\text{Mg}$ values observed in the green jadeitites and amphibole-rich blackwalls indicate that such metasomatism could result in significantly low $\delta^{26}\text{Mg}$ signatures in these rocks. Therefore, coupled dissolution of Ca-rich carbonates and metasomatism by fluid-mediated reactions could deliver carbon to the forearc mantle, thus generating Mg isotope heterogeneity. Our study further indicates that carbon cycling in forearc regions can be constrained by Mg isotopes.

6. Conclusions

The Myanmar jadeitites and country rocks record the fluid-mediated transfer of Mg from an oceanic subduction channel to the mantle wedge. The $\delta^{26}\text{Mg}$ values of jadeitites range from -1.55‰ to -0.74‰ , which are considerably lower than those in oceanic crust and mantle peridotite. The amphibole-rich blackwalls formed by the metasomatism between jadeite-forming fluids and serpentinites systematically exhibit low $\delta^{26}\text{Mg}$ signatures. All of these features indicate that the jadeite-forming fluids have low $\delta^{26}\text{Mg}$ values, which are best explained by the dissolution of Ca-rich carbonates in the fluids at the slab-mantle interface. Metasomatic interactions between such fluids and Cr-rich spinel could increase the $\delta^{26}\text{Mg}$ values in the green jadeitites. Our study suggests that subduction zone fluids dissolving carbonate at forearc depths may have low $\delta^{26}\text{Mg}$ values and that the open-system metasomatism by carbonated fluids along conduits could locally decrease the $\delta^{26}\text{Mg}$ of the forearc mantle wedge.

Acknowledgments

We thank Than Zaw for the help with field excursion. We are grateful to P. Pogge von Strandmann, Wei Yang, Tatsuki Tsujimori, Qiu-Li Li, Jian Huang, and Yi-Xiang Chen for inspiring discussions on the early draft. We thank two anonymous reviewers for their constructive comments and Michael Walter and John Lassiter for careful editorial handling. Mao Q., Ma Y. G., and Yang S. H. are thanked for their help with the mineral major element and bulk-rock composition analyses. This study was financially supported by funds from the National Science Foundation of China (41490614 and 41822202), the International Partnership Program (GJHZ1776), and the Chinese Academy of Sciences (XDB18000000). This paper is dedicated in memoriam to my respectable supervisor Kai Ye. The data for this paper are available via the supporting information and cited references.

References

- Ague, J. J., & Nicolescu, S. (2014). Carbon dioxide released from subduction zones by fluid-mediated reactions. *Nature Geoscience*, 7, 355–360. <https://doi.org/10.1038/ngeo2143>
- Alt, J. C., & Teagle, D. A. H. (1999). Uptake of carbon during alteration of oceanic crust. *Geochimica et Cosmochimica Acta*, 63, 1527–1535. [https://doi.org/10.1016/S0016-7037\(99\)00123-4](https://doi.org/10.1016/S0016-7037(99)00123-4)
- An, Y., Wu, F., Xiang, Y., Nan, X., Yu, X., Yang, J., et al., et al. (2014). High-precision Mg isotope analyses of low-Mg rocks by MC-ICP-MS. *Chemical Geology*, 390, 9–21. <https://doi.org/10.1016/j.chemgeo.2014.09.014>
- Arai, S. (1982). Chemistry of chromian spinel in volcanic rocks as a potential guide to magma chemistry. *Mineralogical Magazine*, 56, 173–184. <https://doi.org/10.1180/minmag.1992.056.383.04>
- Arai, S., Ishimaru, S., & Mizukami, T. (2012). Methane and propane micro-inclusions in olivine in titanoclinohumite-bearing dunites from the Sanbagawa high-P metamorphic belt, Japan: Hydrocarbon activity in a subduction zone and Ti mobility. *Earth and Planetary Science Letters*, 353–354, 1–11. <https://doi.org/10.1016/j.epsl.2012.07.043>
- Arai, S., Okamura, H., Kadoshima, K., Tanaka, C., Suzuki, K., & Ishimaru, S. (2011). Chemical characteristics of chromian spinel in plutonic rocks: Implications for deep magma processes and discrimination of tectonic setting. *Island Arc*, 20, 125–137. <https://doi.org/10.1111/j.1440-1738.2010.00747.x>
- Barnes, S. J., & Roeder, P. L. (2001). The range of spinel compositions in terrestrial mafic and ultramafic rocks. *Journal of Petrology*, 42, 2279–2302. <https://doi.org/10.1093/ptrology/42.12.2279>
- Bebout, G. E. (2013). Metasomatism in subduction zones of subducted oceanic slabs, mantle wedges, and the slab-mantle interface. In D. Harlov, & H. Austrheim (Eds.), *Metasomatism and the chemical transformation of rock, The Role of Fluids in Terrestrial and Extraterrestrial Processes*, (pp. 289–349). Berlin Heidelberg: Springer-Verlag.
- Bebout, G. E., & Penniston-Dorland, S. C. (2016). Fluid and mass transfer at subduction interface—The field metamorphic record. *Lithos*, 240–243, 228–258. <https://doi.org/10.1016/j.lithos.2015.10.007>
- Beinlich, A., Mavromatis, V., Austrheim, H., & Oelkers, E. H. (2014). Inter-mineral Mg isotope fractionation during hydrothermal ultramafic rock alteration—Implications for the global Mg-cycle. *Earth and Planetary Science Letters*, 392, 166–176. <https://doi.org/10.1016/j.epsl.2014.02.028>
- Bender, F. (1983). *Geology of Burma*, (p. 260). Berlin: Gebrüder Bornträger.
- Bertrand, G., Rangin, C., Maluski, H., Han, T. A., Thein, M., Myint, O., et al. (1999). Cenozoic metamorphism along the Shan scarp (Myanmar): Evidence for ductile shear along the Sagaing fault or the northward migration of the eastern Himalayan syntaxis. *Geophysical Research Letters*, 26, 915–918. <https://doi.org/10.1029/1999GL900136>

- Bourdon, B., Tipper, E. T., Fitoussi, C., & Stracke, A. (2010). Chondritic Mg isotope composition of the Earth. *Geochimica et Cosmochimica Acta*, 74, 5069–5083. <https://doi.org/10.1016/j.gca.2010.06.008>
- Brenot, A., Cloquet, C., Vigier, N., Carignan, J., & France-Lanord, C. (2008). Magnesium isotope systematics of the lithologically varied Moselle river basin, France. *Geochimica et Cosmochimica Acta*, 72, 5070–5089. <https://doi.org/10.1016/j.gca.2008.07.027>
- Burkhard, D. J. M. (1993). Accessory chromium spinels: Their coexistence and alteration in serpentinites. *Geochimica et Cosmochimica Acta*, 57, 1297–1306. [https://doi.org/10.1016/0016-7037\(93\)90066-6](https://doi.org/10.1016/0016-7037(93)90066-6)
- Caciagli, N. C., & Manning, C. E. (2003). The solubility of calcite in water at 6–16 kbar and 500–800°C. *Contributions to Mineralogy and Petrology*, 146, 275–285. <https://doi.org/10.1007/s00410-003-0501-y>
- Chen, Y. X., Schertl, H. P., Zheng, Y. F., Huang, F., Zhou, K., & Gong, Y. Z. (2016). Mg–O isotopes trace the origin of Mg-rich fluids in the deeply subducted continental crust of Western Alps. *Earth and Planetary Science Letters*, 456, 157–167. <https://doi.org/10.1016/j.epsl.2016.09.010>
- Collins, N. C., Bebout, G. E., Angiboust, S., Agard, P., Scambelluri, M., Crispini, L., & et al. (2015). Subduction-zone metamorphic pathway for deep carbon cycling: II. Evidence from HP/UHP metabasaltic rocks and ophicarbonates. *Chemical Geology*, 412, 132–150. <https://doi.org/10.1016/j.chemgeo.2015.06.012>
- Dasgupta, R., & Hirschmann, M. M. (2010). The deep carbon cycle and melting in Earth's interior. *Earth and Planetary Science Letters*, 298, 1–13. <https://doi.org/10.1016/j.epsl.2010.06.039>
- Deschamps, F., Godard, M., Guillot, S., & Hattori, K. (2013). Geochemistry of subduction zone serpentinites: A review. *Lithos*, 178, 96–127. <https://doi.org/10.1016/j.lithos.2013.05.019>
- Dick, H. J. B., & Bullen, T. (1984). Chromian spinel as a petrogenetic indicator in abyssal and alpine-type peridotites and spatially associated lavas. *Contributions to Mineralogy and Petrology*, 86, 54–76. <https://doi.org/10.1007/BF00373711>
- Dvir, O., Pettke, T., Fumagalli, P., & Kessel, R. (2011). Fluids in the peridotite–water system up to 6 GPa and 800 °C: New experimental constraints on dehydration reactions. *Contributions to Mineralogy and Petrology*, 161, 829–844. <https://doi.org/10.1007/s00410-010-0567-2>
- Elliott, T. (2003). Tracers of the slab. In J. Eiler (Ed.), *Inside the subduction factory*, *Geophysical Monograph Series*, (Vol. 138, pp. 23–45). Washington, DC: AGU. <https://doi.org/10.1029/138GM03>
- Elliott, T., Plank, T., Zindler, A., White, W., & Bourdon, B. (1997). Element transport from slab to volcanic front at the Mariana arc. *Journal of Geophysical Research*, 102, 14,991–15,019.
- Fantle, M. S., & Higgins, J. (2014). The effects of diagenesis and dolomitization on Ca and Mg isotopes in marine platform carbonates: Implications for the geochemical cycles of Ca and Mg. *Geochimica et Cosmochimica Acta*, 142, 458–481. <https://doi.org/10.1016/j.gca.2014.07.025>
- Galvez, M. E., Manning, C. E., Connolly, J. A. D., & Rumble, D. (2015). The solubility of rocks in metamorphic fluids: A model for rock-dominated conditions to upper mantle pressure and temperature. *Earth and Planetary Science Letters*, 430, 486–498. <https://doi.org/10.1016/j.epsl.2015.06.019>
- Geske, A., Goldstein, R. H., Mavromatis, V., Richter, D. K., Buhl, D., Kluge, T., et al., et al. (2014). The magnesium isotope ($\delta^{26}\text{Mg}$) signature of dolomites. *Geochimica et Cosmochimica Acta*, 149, 131–151. <https://doi.org/10.1016/j.gca.2014.11.003>
- Goffé, B., Rangin, C., & Maluski, H. (2000). Jade and associated rocks from jade mines area, northern Myanmar as record of a polyphased high-pressure metamorphism. *Eos*, 81, F1365.
- Gorman, P. J., Kerrick, D. M., & Connolly, J. A. D. (2006). Modeling open system metamorphic decarbonation of subducting slabs. *Geochemistry, Geophysics, Geosystems*, 7, Q04007. <https://doi.org/10.1029/2005GC001125>
- Guillot, S., Hattori, K., Agard, P., Schwartz, S., & Vidal, O. (2009). Exhumation processes in oceanic and continental subduction contexts: A review. In S. Lallemand, & F. Funiciello (Eds.), *Subduction zone geodynamics*, (pp. 175–205). Berlin Heidelberg: Springer-Verlag. https://doi.org/10.1007/978-3-540-87974-9_10
- Handler, M. R., Baker, J. A., Schiller, M., Bennett, V. C., & Yaxley, G. M. (2009). Magnesium stable isotope composition of Earth's upper mantle. *Earth and Planetary Science Letters*, 282, 306–313. <https://doi.org/10.1016/j.epsl.2009.03.031>
- Harlow, G. E., Flores, K. E., & Marschall, H. R. (2016). Fluid-mediated mass transfer from a paleosubduction channel to its mantle wedge: Evidence from jadeitite and related rocks from the Guatemala Suture Zone. *Lithos*, 258–259, 15–36. <https://doi.org/10.1016/j.lithos.2016.04.010>
- Harlow, G. E., Tsujimori, T., & Sorensen, S. S. (2015). Jadeitites and plate tectonics. *Annual Review of Earth and Planetary Sciences*, 43, 105–138. <https://doi.org/10.1146/annurev-earth-060614-105215>
- Hattori, K. H., & Guillot, S. (2007). Geochemical character of serpentinites associated with high- to ultrahigh-pressure metamorphic rocks in the Alps, Cuba, and the Himalayas: Recycling of elements in subduction zones. *Geochemistry, Geophysics, Geosystems*, 8, Q09010. <https://doi.org/10.1029/2007GC001594>
- Hermann, J., Spandler, C., Hack, A., & Korsakov, A. (2006). Aqueous fluids and hydrous melts in high-pressure and ultra-high pressure rocks: Implications for element transfer in subduction zones. *Lithos*, 92, 399–417. <https://doi.org/10.1016/j.lithos.2006.03.055>
- Higgins, J. A., & Schrag, D. P. (2010). Constraining magnesium cycling in marine sediments using magnesium isotopes. *Geochimica et Cosmochimica Acta*, 74, 5039–5053. <https://doi.org/10.1016/j.gca.2010.05.019>
- Hippler, D., Buhl, D., Witbaard, R., Richter, D. K., & Immenhauser, A. (2009). Towards a better understanding of magnesium-isotope ratios from marine skeletal carbonates. *Geochimica et Cosmochimica Acta*, 73, 6134–6146. <https://doi.org/10.1016/j.gca.2009.07.031>
- Hofmann, A. W. (1997). Mantle geochemistry: The message from oceanic volcanism. *Nature*, 385, 219–229. <https://doi.org/10.1038/385219a0>
- Hu, Y., Teng, F.-Z., Plank, T., & Huang, H.-J. (2017). Magnesium isotopic composition of subducting marine sediments. *Chemical Geology*, 466, 15–31. <https://doi.org/10.1016/j.chemgeo.2017.06.010>
- Huang, F., Chakraborty, P., Lundstrom, C. C., Holmden, C., Glessner, J. J. G., Kieffer, S. W., & et al. (2010). Isotope fractionation in silicate melts by thermal diffusion. *Nature*, 464, 396–400. <https://doi.org/10.1038/nature08840>
- Huang, F., Lundstrom, C. C., Glessner, J., Ianno, A., Boudreau, A., Li, J., et al., et al. (2009). Chemical and isotopic fractionation of wet andesite in a temperature gradient: Experiments and models suggesting a new mechanism of magma differentiation. *Geochimica et Cosmochimica Acta*, 73, 729–749. <https://doi.org/10.1016/j.gca.2008.11.012>
- Huang, F., Zhang, Z., Lundstrom, C. C., & Zhi, X. (2011). Iron and magnesium isotopic compositions of peridotite xenoliths from Eastern China. *Geochimica et Cosmochimica Acta*, 75, 3318–3334. <https://doi.org/10.1016/j.gca.2011.03.036>
- Huang, J., Ke, S., Gao, Y. J., Xiao, Y. L., & Li, S. G. (2015). Magnesium isotopic compositions of altered oceanic basalts and gabbros from IODP site 1256 at the East Pacific Rise. *Lithos*, 231, 53–61. <https://doi.org/10.1016/j.lithos.2015.06.009>
- Huang, J., Li, S. G., Xiao, Y., Ke, S., Li, W. Y., & Tian, Y. (2015). Origin of low $\delta^{26}\text{Mg}$ Cenozoic basalts from South China Block and their geodynamic implications. *Geochimica et Cosmochimica Acta*, 164, 298–317. <https://doi.org/10.1016/j.gca.2015.04.054>
- Huang, J., & Xiao, Y. L. (2016). Mg–Sr isotopes of low- $\delta^{26}\text{Mg}$ basalts tracing recycled carbonate species: Implication for the initial melting depth of the carbonated mantle in Eastern China. *International Geology Review*, 58, 1350–1362. <https://doi.org/10.1080/00206814.2016.1157709>

- Huang K.-J. (2013). The behavior of magnesium isotopes during low-temperature water–rock interactions (PhD dissertation). China University of Geosciences, Wuhan, China.
- Hyndman, R. D., & Peacock, S. M. (2003). Serpentinization of the forearc mantle. *Earth and Planetary Science Letters*, *212*, 417–432. [https://doi.org/10.1016/S0012-821X\(03\)00263-2](https://doi.org/10.1016/S0012-821X(03)00263-2)
- Ishii, T., Robinson, P. T., Maekawa, H., & Fiske, R. (1992). Petrological studies of peridotites from diapiric serpentinite seamounts in the Izu–Ogasawara–Mariana forearc, Leg 125. In P. Fryer, J. A. Pearce, & L. B. Stokking (Eds.), *Proceedings of the Ocean Drilling Program, Scientific Results* (Vol. 125, pp. 445–485). College Station: Ocean Drilling Program.
- Ishwar-Kumar, C., Rajesh, V. J., Windley, B. F., Razakamanana, T., Itaya, T., Babu, E. V. S. S. K., & et al. (2016). Petrogenesis and tectonic setting of the Bondla mafic-ultramafic complex, western India: Inferences from chromian spinel chemistry. *Journal of Asian Earth Sciences*, *130*, 192–205. <https://doi.org/10.1016/j.jseas.2016.07.004>
- Jacobson, A. D., Zhang, Z., Lundstrom, C., & Huang, F. (2010). Behavior of Mg isotopes during dedolomitization in the Madison Aquifer, South Dakota. *Earth and Planetary Science Letters*, *297*, 446–452. <https://doi.org/10.1016/j.epsl.2010.06.038>
- John, T., Klemm, R., Gao, J., & Garbe-Schönberg, C. D. (2008). Trace-element mobilization in slabs due to non steady-state fluid–rock interaction: Constraints from an eclogite facies transport vein in blueschist (Tianshan, China). *Lithos*, *103*, 1–24. <https://doi.org/10.1016/j.lithos.2007.09.005>
- Kasemann, S. A., Pogge von Strandmann, P. A. E., Prave, A. R., Fallick, A. E., Elliott, T., & Hoffmann, K. H. (2014). Continental weathering following a Cryogenian glaciation: Evidence from calcium and magnesium isotopes. *Earth and Planetary Science Letters*, *396*, 66–77. <https://doi.org/10.1016/j.epsl.2014.03.048>
- Kelemen, P. B., & Manning, C. E. (2015). Reevaluating carbon fluxes in subduction zones, what goes down, mostly comes up. *Proceedings of the National Academy of Sciences*, *112*(30), E3997–E4006. <https://doi.org/10.1073/pnas.1507889112>
- Kerrick, D. M., & Connolly, J. A. D. (1998). Subduction of ophicarbonates and recycling of CO₂ and H₂O. *Geology*, *26*(4), 375–378.
- Kerrick, D. M., & Connolly, J. A. D. (2001). Metamorphic devolatilization of subducted marine sediments and the transport of volatiles into the Earth's mantle. *Nature*, *411*, 293–296.
- Kessel, R., Ulmer, P., Pettke, T., Schmidt, M. W., & Thompson, A. B. (2005). The water–basalt system at 4 to 6 GPa: Phase relations and second critical endpoint in a K-free eclogite at 700 to 1400 °C. *Earth and Planetary Science Letters*, *237*, 873–892. <https://doi.org/10.1016/j.epsl.2005.06.018>
- Kimball, K. L. (1990). Effects of hydrothermal alteration on the compositions of chromian spinels. *Contributions to Mineralogy and Petrology*, *105*, 337–346. <https://doi.org/10.1007/BF00306543>
- King, R. L., Bebout, G. E., Moriguti, T., & Nakamura, E. (2006). Elemental mixing systematics and Sr–Nd isotope geochemistry of mélange formation: Obstacles to identification of fluid sources to arc volcanics. *Earth and Planetary Science Letters*, *246*, 288–304. <https://doi.org/10.1016/j.epsl.2006.03.053>
- Lazar, C., Zhang, C., Manning, C. E., & Mysen, B. O. (2014). Redox effects on calcite–portlandite–fluid equilibria at forearc conditions: Carbon mobility, methanogenesis, and reduction melting of calcite. *American Mineralogist*, *99*, 1604–1615. <https://doi.org/10.2138/am.2014.4696>
- Lei, W. Y., Shi, G. H., Santosh, M., Ng, Y., Liu, Y. X., Wang, J., et al. (2016). Trace element features of hydrothermal and inherited igneous zircon grains in mantle wedge environment: A case study from the Myanmar jadeitite. *Lithos*, *266–267*, 16–27. <https://doi.org/10.1016/j.lithos.2016.09.031>
- Li, S. G., Yang, W., Ke, S., Meng, X., Tian, H. C., Xu, L. J., et al. (2017). Deep carbon cycles constrained by a large-scale mantle Mg isotope anomaly in eastern China. *National Science Review*, *4*, 111–120. <https://doi.org/10.1093/nsr/nww070>
- Li, W. Q., Beard, B. L., Li, C., & Johnson, C. M. (2014). Magnesium isotope fractionation between brucite [Mg(OH)₂] and Mg aqueous species: Implications for silicate weathering and biogeochemical processes. *Earth and Planetary Science Letters*, *394*, 82–93. <https://doi.org/10.1016/j.epsl.2014.03.022>
- Li, W. Y., Teng, F. Z., Wing, B. A., & Xiao, Y. L. (2014). Limited magnesium isotope fractionation during metamorphic dehydration in metapelites from the Onawa contact aureole, Maine. *Geochemistry, Geophysics, Geosystems*, *15*, 408–415. <https://doi.org/10.1002/2013GC004992>
- Li, W. Y., Teng, F. Z., Xiao, Y., & Huang, J. (2011). High-temperature inter-mineral magnesium isotope fractionation in eclogite from the Dabie orogen, China. *Earth and Planetary Science Letters*, *304*, 224–230. <https://doi.org/10.1016/j.epsl.2011.01.035>
- Ling, M. X., Sedaghatpour, F., Teng, F. Z., Hays, P. D., Strauss, J., & Sun, W. (2011). Homogeneous magnesium isotopic composition of seawater: An excellent geostandard for Mg isotope analysis. *Rapid Communications in Mass Spectrometry*, *25*, 2828–2836. <https://doi.org/10.1002/rcm.5172>
- Liu, C. Z., Zhang, C., Xu, Y., Wang, J. G., Chen, Y., Guo, S., et al. (2016). Petrology and geochemistry of mantle peridotites from the Kalaymyo and Myitkyina ophiolites (Myanmar): Implications for tectonic settings. *Lithos*, *264*, 495–508. <https://doi.org/10.1016/j.lithos.2016.09.013>
- Liu, D., Zhao, Z., Zhu, D.-C., Niu, Y., Widom, E., Teng, F.-Z., et al. (2015). Identifying mantle carbonatite metasomatism through Os–Sr–Mg isotopes in Tibetan ultrapotassic rocks. *Earth and Planetary Science Letters*, *430*, 458–469. <https://doi.org/10.1016/j.epsl.2015.09.005>
- Liu, P. P., Teng, F. Z., Dick, H. J. B., Zhou, M. F., & Chung, S. L. (2017). Magnesium isotopic composition of the oceanic mantle and oceanic Mg cycling. *Geochimica et Cosmochimica Acta*, *206*, 151–165. <https://doi.org/10.1016/j.gca.2017.02.016>
- Liu, S. A., Teng, F. Z., He, Y., Ke, S., & Li, S. G. (2010). Investigation of magnesium isotope fractionation during granite differentiation: Implication for Mg isotopic composition of the continental crust. *Earth and Planetary Science Letters*, *297*, 646–654. <https://doi.org/10.1016/j.epsl.2010.07.019>
- Manning, C. E. (2004). The chemistry of subduction-zone fluids. *Earth and Planetary Science Letters*, *223*, 1–16. <https://doi.org/10.1016/j.epsl.2004.04.030>
- Manning, C. E. (2013). Thermodynamic modeling of fluid–rock interaction at mid-crustal to upper-mantle conditions. *Reviews in Mineralogy and Geochemistry*, *76*, 135–164. <https://doi.org/10.2138/rmg.2013.76.5>
- Manning, C. E., Antignano, A., & Lin, H. A. (2010). Premelting polymerization of crustal and mantle fluids, as indicated by the solubility of albite + paragonite + quartz in H₂O at 1 GPa and 350–620 °C. *Earth and Planetary Science Letters*, *292*, 325–336. <https://doi.org/10.1016/j.epsl.2010.01.044>
- Manning, C. E., Shock, E. L., & Sverjensky, D. A. (2013). The chemistry of carbon in aqueous fluids at crustal and upper-mantle conditions: Experimental and theoretical constraints. *Reviews in Mineralogy and Geochemistry*, *75*, 109–148. <https://doi.org/10.2138/rmg.2013.75.5>
- Marschall, H. R., & Schumacher, J. C. (2012). Arc magmas sourced from mélange diapirs in subduction zones. *Nature Geoscience*, *5*, 862–867. <https://doi.org/10.1038/ngeo1634>
- Mével, C., & Kiänast, J. R. (1986). Jadeite–kosmochlor solid solution and chromian sodic amphiboles in jadeitites and associated rocks from Tawmaw (Burma). *Bulletin de Mineralogie*, *109*, 617–633.

- Mitchell, A., Chung, S. L., Oo, T., Lin, T. H., & Hung, C. H. (2012). Zircon U-Pb ages in Myanmar: Magmatic-metamorphic events and the closure of a neo-Tethys ocean? *Journal of Asian Earth Sciences*, *56*, 1–23. <https://doi.org/10.1016/j.jseas.2012.04.019>
- Mitchell, A. H. G., Htay, M. T., Htun, K. M., Win, M. N., Oo, T., & Hlaing, T. (2007). Rock relationships in the Mogok Metamorphic Belt, Tatkon to Mandalay, Central Myanmar. *Journal of Asian Earth Sciences*, *29*, 891–910. <https://doi.org/10.1016/j.jseas.2006.05.009>
- Molina, J. F., & Poli, S. (2000). Carbonate stability and fluid composition in subducted oceanic crust: An experimental study on H₂O–CO₂-bearing basalts. *Earth and Planetary Science Letters*, *176*, 295–310. [https://doi.org/10.1016/S0012-821X\(00\)00021-2](https://doi.org/10.1016/S0012-821X(00)00021-2)
- Morris, J. D., & Ryan, J. G. (2003). Subduction zone processes and implications for changing composition of the upper and lower mantle. *Treatise on Geochemistry*, *2*, 451–470. <https://doi.org/10.1016/B0-08-043751-6/02011-9>
- Newton, R. C., & Manning, C. E. (2002). Experimental determination of calcite solubility in H₂O–NaCl solutions at deep crust/upper mantle pressures and temperatures: Implications for metasomatic processes in shear zones. *American Mineralogist*, *87*, 1401–1409. <https://doi.org/10.2138/am-2002-1016>
- Ng, Y. N., Shi, G. H., & Santosh, M. (2016). Titanite-bearing omphacite from the jade tract, Myanmar: Interpretation from mineral and trace element compositions. *Journal of Asian Earth Sciences*, *117*, 1–12. <https://doi.org/10.1016/j.jseas.2015.12.011>
- Nozaka, T. (2003). Compositional heterogeneity of olivine in thermally metamorphosed serpentinite from southwest Japan. *American Mineralogist*, *88*, 1377–1384. <https://doi.org/10.2138/am-2003-8-922>
- Nyunt, T. T. (2009). Petrological and geochemical contribution to the origin of jadeite and associated rocks of the Tawmaw Area, Kachin State, Myanmar. Doctoral Dissertation Institut für Mineralogie und Kristallchemie der Universität Stuttgart.
- Pan, D., Spanu, L., Harrison, B., Sverjensky, D. A., & Galli, G. (2013). Dielectric properties of water under extreme conditions and transport of carbonates in the deep Earth. *Proceedings of the National Academy of Sciences*, *110*(7), 6646–6650. <https://doi.org/10.1073/pnas.1221581110>
- Pearce, J. A., Barker, P. F., Edwards, S. J., Parkinson, I. J., & Leat, P. T. (2000). Geochemistry and tectonic significance of peridotites from the South Sandwich arc-basin system, South Atlantic. *Contributions to Mineralogy and Petrology*, *139*, 36–53.
- Penniston-Dorland, S. C., Kohn, M. J., & Manning, C. E. (2015). The global range of subduction zone thermal structures from exhumed blueschists and eclogites: Rocks are hotter than models. *Earth and Planetary Science Letters*, *428*, 243–254. <https://doi.org/10.1016/j.epsl.2015.07.031>
- Plank, T., & Langmuir, C. H. (1993). Tracing trace elements from sediment input to volcanic output at subduction zones. *Nature*, *362*, 739–743.
- Plümpner, O., John, T., Podladchikov, Y. Y., Vrijmoed, C., & Scambelluri, M. (2017). Fluid escape from subduction zones controlled by channel-forming reactive porosity. *Nature Geoscience*, *10*, 150–156. <https://doi.org/10.1038/ngeo2865>
- Pogge von Strandmann, P. A. E., Dohmen, R., Marschall, H. R., Schumacher, J. C., & Elliott, T. (2015). Extreme magnesium isotope fractionation at outcrop scale records the mechanism and rate at which reaction fronts advance. *Journal of Petrology*, *56*, 33–58. <https://doi.org/10.1093/ptrology/egu070>
- Pogge von Strandmann, P. A. E., Elliott, T., Marschall, H. R., Coath, C., Lai, Y. J., Jeffcoate, A. B., & et al. (2011). Variations of Li and Mg isotope ratios in bulk chondrites and mantle xenoliths. *Geochimica et Cosmochimica Acta*, *75*, 5247–5268. <https://doi.org/10.1016/j.gca.2011.06.026>
- Poli, S., Franzolin, E., Fumagalli, P., & Crottini, A. (2009). The transport of carbon and hydrogen in subducted oceanic crust: An experimental study to 5 GPa. *Earth and Planetary Science Letters*, *278*, 350–360. <https://doi.org/10.1016/j.epsl.2008.12.022>
- Qi, M., Shen, K., & Xiang, H. (2015). Fluid inclusions in the Myanmar jadeiteites. *Acta Petrologica et Mineralogica*, *34*, 405–417.
- Qiu, Z. L., Wu, F. Y., Yang, S. F., Zhu, M., Sun, J. F., & Yang, P. (2009). Age and genesis of the Myanmar jadeite: Constraints from U–Pb ages and Hf isotopes of zircon inclusions. *Chinese Science Bulletin*, *54*, 658–668. <https://doi.org/10.1007/s11434-008-0490-3>
- Richter, F. M., Davis, A. M., DePaolo, D. J., & Watson, E. B. (2003). Isotope fractionation by chemical diffusion between molten basalt and rhyolite. *Geochimica et Cosmochimica Acta*, *67*, 3905–3923. [https://doi.org/10.1016/S0016-7037\(03\)00174-1](https://doi.org/10.1016/S0016-7037(03)00174-1)
- Scambelluri, M., Bebout, G. E., Belmonte, D., Gillio, M., Campomenosi, N., Collins, N., & et al. (2016). Carbonation of subduction-zone serpentinite (high-pressure ophicarbonates; Ligurian Western Alps) and implications for the deep carbon cycling. *Earth and Planetary Science Letters*, *441*, 155–166. <https://doi.org/10.1016/j.epsl.2016.02.034>
- Scambelluri, M., Fiebig, J., Malaspina, N., Müntener, O., & Pettko, T. (2004). Serpentinite subduction: Implications for fluid processes and trace-element recycling. *International Geology Review*, *46*, 595–613. <https://doi.org/10.2747/0020-6814.46.7.595>
- Scambelluri, M., Pettko, T., & Cannàò, E. (2015). Fluid-related inclusions in Alpine high-pressure peridotite reveal trace element recycling during subduction-zone dehydration of serpentinitized mantle (Cima di Gagnone, Swiss Alps). *Earth and Planetary Science Letters*, *429*, 45–59. <https://doi.org/10.1016/j.epsl.2015.07.060>
- Scambelluri, M., & Tonarini, S. (2012). Boron isotope evidence for shallow fluid transfer across subduction zones by serpentinitized mantle. *Geology*, *40*, 907–910. <https://doi.org/10.1130/G33233.1>
- Schauble, E. A. (2011). First-principles estimates of equilibrium magnesium isotope fractionation in silicate, oxide, carbonate and hexaaquamagnesium (2+) crystals. *Geochimica et Cosmochimica Acta*, *75*, 844–869. <https://doi.org/10.1016/j.gca.2010.09.044>
- Schertl, H. P., Maresch, W. V., Stanek, K. P., Hertwig, A., Krebs, M., Baese, R., & et al. (2012). New occurrences of jadeite, jadeite quartzite and jadeite-lawsonite quartzite in the Dominican Republic, Hispaniola: Petrological and geochronological overview. *European Journal of Mineralogy*, *24*(2), 199–216. <https://doi.org/10.1127/0935-1221/2012/0024-2201>
- Schmidt, M. W., & Poli, S. (1998). Experimentally based water budgets for dehydrating slabs and consequences for arc magma generation. *Earth and Planetary Science Letters*, *163*, 361–379. [https://doi.org/10.1016/S0012-821X\(98\)00142-3](https://doi.org/10.1016/S0012-821X(98)00142-3)
- Schneider, M. E., & Eggler, D. H. (1986). Fluids in equilibrium with peridotite minerals: Implications for mantle metasomatism. *Geochimica et Cosmochimica Acta*, *50*, 711–724. [https://doi.org/10.1016/0016-7037\(86\)90347-9](https://doi.org/10.1016/0016-7037(86)90347-9)
- Searle, M. P., Nobel, S. R., Cottle, J. M., Waters, D. J., Mitchell, A. H. G., Hlaing, T., & et al. (2007). Tectonic evolution of the Mogok metamorphic belt, Burma (Myanmar) constrained by U–Th–Pb dating of metamorphic and magmatic rocks. *Tectonics*, *26*, TC3014. <https://doi.org/10.1029/2006TC002083>
- Sharp, Z. D., & Barnes, J. D. (2004). Water-soluble chlorides in massive seafloor serpentinites: A source of chloride in subduction zones. *Earth and Planetary Science Letters*, *226*, 243–254. <https://doi.org/10.1016/j.epsl.2004.06.016>
- Shi, G. H., Cui, W. Y., Cao, S. M., Jiang, N., Jian, P., Liu, D. Y., et al. (2008). Ion microprobe zircon U–Pb age and geochemistry of the Myanmar jadeite. *Journal of Geological Society*, *165*, 221–234. <https://doi.org/10.1144/0016-76492006-119>
- Shi, G. H., Cui, W. Y., Liu, J., & Yu, H. Y. (2001). The petrology of jadeite-bearing serpentinitized peridotite and its country rocks from Northwestern Myanmar (Burma). *Acta Petrologica Sinica*, *17*, 483–490.
- Shi, G. H., Cui, W. Y., Tropper, P., Wang, C. Q., Shu, G. M., & Yu, H. X. (2003). The petrology of a complex sodic and sodic–calcic amphibole association and its implications for the metasomatic processes in the jadeite area in northwestern Myanmar, formerly Burma. *Contributions to Mineralogy and Petrology*, *145*, 355–376. <https://doi.org/10.1007/s00410-003-0457-y>

- Shi, G. H., Harlow, G. E., Wang, J., Ng, E., Wang, X., Cao, S. M., & et al. (2012). Mineralogy of jadeite and related rocks from Myanmar: A review with new data. *European Journal of Mineralogy*, 24, 345–370. <https://doi.org/10.1127/0935-1221/2012/0024-2190>
- Shi, G. H., Jiang, N., Liu, Y., Wang, X., Zhang, Z. Y., & Xu, Y. J. (2009). Zircon Hf isotope signature of the depleted mantle in the Myanmar jadeite: Implications for Mesozoic intra-oceanic subduction between the Eastern Indian Plate and the Burmese Platelet. *Lithos*, 112, 342–350. <https://doi.org/10.1016/j.lithos.2009.03.011>
- Shi, G. H., Jiang, N., Wang, Y. W., Zhao, X., Wang, X., Li, G. W., et al., et al. (2010). Ba minerals in clinopyroxene rocks from the Myanmar jadeite area: Implications for Ba recycling in subduction zones. *European Journal of Mineralogy*, 22, 199–214. <https://doi.org/10.1127/0935-1221/2010/0022-1998>
- Shi, G. H., Lei, W. Y., He, H. Y., Ng, Y. N., Liu, Y., Liu, X. Y., et al., et al. (2014). Superimposed tectono-metamorphic episodes of Jurassic and Eocene age in the jadeite uplift, Myanmar, as revealed by $^{40}\text{Ar}/^{39}\text{Ar}$ dating. *Gondwana Research*, 26, 464–474. <https://doi.org/10.1016/j.gr.2013.08.007>
- Shi, G. H., Stöckhert, B., & Cui, W. Y. (2005). Kosmochlor and chromian jadeite aggregates from Myanmar area. *Mineralogical Magazine*, 69, 1059–1075. <https://doi.org/10.1180/0026461056960308>
- Shi, G. H., Tropper, P., Cui, W. Y., Tian, J., & Wang, C. Q. (2005). Methane (CH₄)-bearing fluid inclusions in Myanmar jadeites. *Geochemical Journal*, 39, 503–516. <https://doi.org/10.2343/geochemj.39.503>
- Shi, G. H., Zhu, X. K., Deng, J., Mao, Q., Liu, Y. X., & Li, G. W. (2011). Spherules with pure iron cores from Myanmar jadeite: type-I deep-sea spherules? *Geochimica et Cosmochimica Acta*, 75, 1608–1620. <https://doi.org/10.1016/j.gca.2011.01.005>
- Song, S. G., Su, L., Niu, Y. L., Lai, Y., & Zhang, L. F. (2009). CH₄ inclusions in orogenic harzburgite: Evidence for reduced slab fluids and implication for redox melting in mantle wedge. *Geochimica et Cosmochimica Acta*, 73, 1737–1754. <https://doi.org/10.1016/j.gca.2008.12.008>
- Sorensen, S. S., Harlow, G. E., & Rumble, D. (2006). The origin of jadeite-forming subduction zone fluids: CL-guided SIMS oxygen isotope and trace element evidence. *American Mineralogist*, 91, 979–996. <https://doi.org/10.2138/am.2006.1949>
- Spandler, C., Mavrogenes, J., & Hermann, J. (2007). Experimental constraints on element mobility from subducted sediments using high-P synthetic fluid/melt inclusions. *Chemical Geology*, 239, 228–249. <https://doi.org/10.1016/j.chemgeo.2006.10.005>
- Spandler, C., Pettker, T., & Hermann, J. (2014). Experimental study of trace element release during ultrahigh-pressure serpentinite dehydration. *Earth and Planetary Science Letters*, 391, 296–306. <https://doi.org/10.1016/j.epsl.2014.02.010>
- Spandler, C., & Pirard, C. (2013). Element recycling from subducting slabs to arc crust: A review. *Lithos*, 170–171, 208–233. <https://doi.org/10.1016/j.lithos.2013.02.016>
- Stalder, R., Ulmer, P., Thompson, A. B., & Gunther, D. (2001). High pressure fluids in the system MgO-SiO₂-H₂O under upper mantle conditions. *Contributions to Mineralogy and Petrology*, 140, 607–618. <https://doi.org/10.1007/s004100000212>
- Syracuse, E. M., van Keken, P. E., & Abers, G. A. (2010). The global range of subduction zone thermal models. *Physics of the Earth and Planetary Interiors*, 51, 1761–1782. <https://doi.org/10.1016/j.pepi.2010.02.004>
- Takahashi, E. (1986). Origin of basaltic magmas-implications from peridotite melting experiments and an olivine fractionation model. *Bulletin of the Volcanological Society of Japan*, 30, 517–540.
- Tatsumi, Y. (1986). Formation of the volcanic front in subduction zones. *Geophysical Research Letters*, 13, 717–720.
- Tatsumi, Y. (1989). Migration of fluid phases and genesis of basalt magmas in subduction zones. *Journal of Geophysical Research*, 94, 4697–4707. <https://doi.org/10.1029/JB094iB04p04697>
- Teng, F. Z. (2017). Magnesium isotope geochemistry. *Reviews in Mineralogy and Geochemistry*, 82, 219–287.
- Teng, F. Z., Hu, Y., & Chauvel, C. (2016). Magnesium isotope geochemistry in arc volcanism. *Proceedings of the National Academy of Sciences*, 113, 7082–7087. <https://doi.org/10.1073/pnas.1518456113>
- Teng, F. Z., Li, W. Y., Ke, S., Marty, B., Dauphas, N., Huang, S., et al., et al. (2010). Magnesium isotopic composition of the Earth and chondrites. *Geochimica et Cosmochimica Acta*, 74, 4150–4166. <https://doi.org/10.1016/j.gca.2010.04.019>
- Thomsen, T. B., & Schmidt, M. W. (2008). The biotite to phengite reaction and mica-dominated melting in fluid carbonate-saturated pelites at high pressures. *Journal of Petrology*, 49, 1889–1914. <https://doi.org/10.1093/petrology/egn051>
- Tian, H. C., Yang, W., Li, S.-G., Ke, S., & Chu, Z. Y. (2016). Origin of low $\delta^{26}\text{Mg}$ basalts with EM-I component: Evidence for interaction between enriched lithosphere and carbonated asthenosphere. *Geochimica et Cosmochimica Acta*, 188, 93–105. <https://doi.org/10.1016/j.gca.2016.05.021>
- Tipper, E., Galy, A., Gaillardet, J., Bickle, M., Elderfield, H., & Carder, E. (2006). The magnesium isotope budget of the modern ocean: Constraints from riverine magnesium isotope ratios. *Earth and Planetary Science Letters*, 250, 241–253. <https://doi.org/10.1016/j.epsl.2006.07.037>
- Tsujiyori, T., & Harlow, G. E. (2012). Petrogenetic relationships between jadeite and associated high-pressure and low-temperature metamorphic rocks in worldwide jadeite localities: A review. *European Journal of Mineralogy*, 24, 371–390. <https://doi.org/10.1127/0935-1221/2012/0024-2193>
- Ulmer, P., & Trommsdorff, V. (1995). Serpentine stability to mantle depths and subduction related magmatism. *Science*, 268, 858–861. <https://doi.org/10.1126/science.268.5212.858>
- Wang, S. J., Teng, F. Z., Li, S. G., & Hong, J. A. (2014). Magnesium isotopic systematics of mafic rocks during continental subduction. *Geochimica et Cosmochimica Acta*, 143, 34–48. <https://doi.org/10.1016/j.gca.2014.03.029>
- Wang, S. J., Teng, F. Z., Li, S. G., Zhang, L. F., Du, J. X., He, Y. S., & et al. (2017). Tracing subduction zone fluid-rock interactions using trace element and Mg-Sr-Nd isotopes. *Lithos*, 290–291, 94–103. <https://doi.org/10.1016/j.lithos.2017.08.004>
- Wang, S. J., Teng, F. Z., Rudnick, R. L., & Li, S. G. (2015). Magnesium isotope evidence for a recycled origin of cratonic eclogites. *Geology*, 43, 1071–1074. <https://doi.org/10.1130/G37259.1>
- Wang, S. J., Teng, F. Z., Williams, H. M., & Li, S. G. (2012). Magnesium isotopic variations in cratonic eclogites: Origins and implications. *Earth and Planetary Science Letters*, 359, 219–226. <https://doi.org/10.1016/j.epsl.2012.10.016>
- Warren, J. M. (2016). Global variations in abyssal peridotite compositions. *Lithos*, 248–251, 193–219. <https://doi.org/10.1016/j.lithos.2015.12.023>
- Whitney, D. L., & Evans, B. W. (2010). Abbreviations for names of rock-forming minerals. *American Mineralogist*, 95, 185–187. <https://doi.org/10.2138/am.2010.3371>
- Wimpenny, J., Colla, C. A., Yin, Q., Rustad, J. R., & Casey, W. H. (2014). Investigating the behavior of Mg isotopes during the formation of clay minerals. *Geochimica et Cosmochimica Acta*, 128, 178–194. <https://doi.org/10.1016/j.gca.2013.12.012>
- Wohlars, A., Manning, C. E., & Thompson, A. B. (2011). Experimental investigation of the solubility of albite and jadeite in H₂O, with paragonite + quartz at 500 and 600 °C, and 1–2.25 GPa. *Geochimica et Cosmochimica Acta*, 75, 2924–2939. <https://doi.org/10.1016/j.gca.2011.02.028>
- Wombacher, F., Eisenhauer, A., Böhm, F., Gussone, N., Regenber, M., Dullo, W. C., & et al. (2011). Magnesium stable isotope fractionation in marine biogenic calcite and aragonite. *Geochimica et Cosmochimica Acta*, 75, 5797–5818. <https://doi.org/10.1016/j.gca.2011.07.017>

- Xiao, Y., Teng, F. Z., Zhang, H. F., & Yang, W. (2013). Large magnesium isotope fractionation in peridotite xenoliths from eastern North China craton: Product of melt–rock interaction. *Geochimica et Cosmochimica Acta*, *115*, 241–261. <https://doi.org/10.1016/j.gca.2013.04.011>
- Yang, J. J., & Powell, R. (2008). Ultrahigh-pressure garnet peridotites from the devolatilization of sea-floor hydrated ultramafic rocks. *Journal of Metamorphic Geology*, *26*, 695–716. <https://doi.org/10.1111/j.1525-1314.2008.00780.x>
- Yang, W., Teng, F. Z., & Zhang, H. F. (2009). Chondritic magnesium isotopic composition of the terrestrial mantle: A case study of peridotite xenoliths from the North China craton. *Earth and Planetary Science Letters*, *288*, 475–482. <https://doi.org/10.1016/j.epsl.2009.10.009>
- Yang, W., Teng, F. Z., Zhang, H. F., & Li, S. G. (2012). Magnesium isotopic systematics of continental basalts from the North China craton: Implications for tracing subducted carbonate in the mantle. *Chemical Geology*, *328*, 185–194. <https://doi.org/10.1016/j.chemgeo.2012.05.018>
- Young, E. D., Tonui, E., Manning, C. E., Schauble, E., & Macris, C. A. (2009). Spinel-olivine magnesium isotope thermometry in the mantle and implications for the Mg isotopic composition of Earth. *Earth and Planetary Science Letters*, *288*, 524–533. <https://doi.org/10.1016/j.epsl.2009.10.014>
- Yui, T. F., Fukuyama, M., Iizuka, Y., Wu, C. M., & Wu, T. W. (2013). Is Myanmar jadeitite of Jurassic age? A result from incompletely recrystallized inherited zircon. *Lithos*, *160–161*, 268–282. <https://doi.org/10.1016/j.lithos.2012.12.011>